Neural Computing and Applications (2023) 35:23649–23665
https://doi.org/10.1007/s00521-023-08980-5

ORIGINAL ARTICLE

Projective lag quasi-synchronization of coupled systems with mixed delays and parameter mismatch: a unified theory

Vipin Kumar[1] · Jan Heiland[1,2] · Peter Benner[1,2]

Received: 8 March 2023 / Accepted: 15 August 2023 / Published online: 11 September 2023

Abstract
This paper investigates the projective lag quasi-synchronization by feedback control of a coupled dynamical system with delays and parameter mismatches on arbitrary time domains. Being formulated on time scales, our results are valid simultaneously for continuous- and discrete-time models as well as for any non-standard time domain. Furthermore, the controller design respects the structure of the equations so that we can characterize the stabilization by a limited controller action. Our proofs rely on the unified matrix-measure theory and the generalized Halanay inequality on time scales. We validate our theoretical results with several simulation examples on various time domains.

Keywords Time scales · Synchronization · Coupled delayed systems · Parameter mismatches · Matrix-measure

1 Introduction

Synchronization is a fundamental property of dynamic systems, where two or more systems achieve a coordinated behaviour, typically through the use of coupling or external forces. It has been an interesting problem since the seminal work of Pecora and Carroll [1] and has applications in many fields of engineering and science, such as image encryption [2], signal and image processing [3], and secure communication [4]. As a result, in the last two decades, many authors have studied the synchronization problem for various types of continuous-time and discrete-time dynamic systems; see, for example, [5–16], and the references cited therein. To establish the synchronization results, the authors mainly used two techniques: one is the Lyapunov technique or functional method, see, for instance, [5–10]. The second technique is based on the direct method or matrix-measure method which comes with a general algebraic approach to stability or stabilizability as opposed to the often problem-specific construction of Lyapunov functions. The stability and synchronization problem using the matrix-measure method has been studied, for example, in [11–15].

In the literature, researchers have developed different types of synchronization schemes such as exponential synchronization [17, 18], quasi-synchronization [19, 20], lag synchronization [21], and projective synchronization [22]. Among these schemes, projective lag synchronization [23] is a scheme that includes both the projective and lag factors. Here, the state of the response system y lags behind the state of the master system x proportionally after a transient time, i.e. $y(t) = \alpha x(t - \varsigma)$, where $\varsigma > 0$ is the lag delay and α is a projective real constant. This scheme has been used in secure communication to extend binary digital to M-nary digital and achieve fast communication [23] and has received more attention in recent years [24–27]. Particularly, in [25], the authors investigated projective lag synchronization in spatiotemporal chaotic systems with disturbances and time delay using the sliding mode control technique. In [26], the finite-time generalized projective lag synchronization of neutral-type neural networks with delay was studied by using the Gronwall–Bellman inequality and nonlinear feedback control. Additionally, [27] addressed

✉ Vipin Kumar
vkumar@mpi-magdeburg.mpg.de

Jan Heiland
heiland@mpi-magdeburg.mpg.de

Peter Benner
benner@mpi-magdeburg.mpg.de

[1] Max Planck Institute for Dynamics of Complex Technical Systems, Sandtorstraße 1, 39106 Magdeburg, Germany

[2] Faculty of Mathematics, Otto von Guericke University Magdeburg, 39106 Magdeburg, Germany

function projective lag synchronization in chaotic systems by utilizing nonlinear adaptive impulsive control and the Lyapunov stability theory.

Further, in many practical applications, parameter mismatches between the drive and response systems are a common issue which can significantly impact the convergence rate of synchronization or even completely prevent synchronization from occurring. Therefore, it is important to establish synchronization results in systems with parameter mismatches. Recently, few authors have investigated the parameter mismatches systems (see, for example, [28–38]). In particular, the authors in Zou et al. [31] proposed two novel protocols for leader–follower and leaderless scenarios using the reference trajectory-based method. They also investigated finite-time consensus in second-order multi-agent systems with non-identical nonlinear dynamics under directed networks by using graph theory, Lyapunov functional method, and finite-time stability theory. In Huang et al. [32] and Yuan et al. [33], the authors discussed the projective lag synchronization and lag quasi-synchronization of coupled systems with parameter mismatch and mixed delays by using the intermittent control and Lyapunov techniques, while in Chen and Cao [34] and He et al. [35], the authors studied the projective synchronization and lag quasi-synchronization results of two coupled delayed systems with parameter mismatch by using the feedback control, generalized Halanay inequality, and matrix-measure method. Additionally, in Huang et al. [36], the authors investigated the weak projective lag synchronization results for coupled neural networks with parameter mismatch and delay by using the feedback control and Lyapunov stability theorem. In Feng and Yang [37], the authors studied the projective lag synchronization results for two different discrete-time chaotic systems by using the feedback controller and Lyapunov method, and in Xiao and Huang [38], the problem of quasi-synchronization for discrete-time inertial neural networks with delay was studied by using the matrix-measure method.

It is worth noting that all the aforementioned results about synchronization have been studied for continuous-time and discrete-time systems but separately. Apart from these separate studies being possibly partially redundant, there exist physical models that consider continuous and discrete evolution at the same time or on some different timelines. For example, in a simple *RLC* circuit (see Fig. 1), a dynamical scenario with a discharge of the capacitor that takes $\delta > 0$ time units and occurs periodically after l time units can conveniently be modelled on the time domain [39]: $T = \cup_{l=0}^{\infty}[l, l+1-\delta]$.

Further, the life span of several species including Pharaoh-Cicada, Magi-Cicada Cassini, and Magi-Cicada

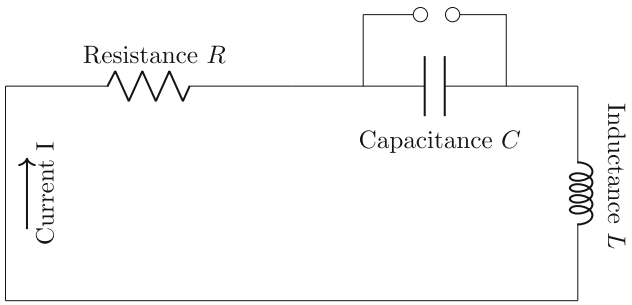

Fig. 1 A simple RLC circuit

Septendecim is represented by the union of equal-length closed time intervals with some gap, i.e. they grow continuously as well as discretely in different stages of their life, and hence, to examine the dynamic properties of these species, one may consider a time domain $T = \cup_{l=0}^{\infty}[l(c+d), l(c+d)+d]$, where $c, d \in \mathbb{R}^+$ [39]. Furthermore, certain neurons in our brain are active during the day and inactive at night, and this process continues with respect to time. The active dynamics of neurons can be intuitively viewed in the time domain $\mathbb{T} = \cup_{l=0}^{\infty}[24l, 24l+d_l]$, where d_l denotes the number of active hours of the neurons in each day (see Fig. 2).

Since these types of models evolve in both continuous- and discrete-time domains, in order to study their dynamic behaviour more accurately, we require a dynamic system that can simultaneously incorporate both continuous and discrete-time domains. In this regard, Hilger [40] introduced the concept of *time scales theory (measure chain theory)*, which unifies, extends, and bridges the conventional continuous and discrete dynamical systems into a single unified theory. The results obtained on time scales are not only applicable to discrete and continuous-time domains but also valid for any hybrid-type time domains (a combination of discrete and continuous-time domain, non-uniform discrete sets) which are useful in the study of various complex dynamical systems. For further study on time scales calculus, see [39, 41].

In recent years, time scales theory has gained significant attention due to its diverse applications in science and engineering, including control theory [42], economics [43], and epidemiology [44]. Qualitative properties of dynamic equations on time scales, such as positivity, observability, controllability, and stability, have been extensively studied (see, for instance, [45–48] and references therein). However, few studies have investigated the synchronization of coupled dynamic systems on time scales [49–56]. Particularly, in Lu et al. [52], synchronization results were investigated for complex dynamical networks with delays on time scales by using the unified Wirtinger-based inequality, while in Ali and Yogambigai [53], global exponential synchronization results of dynamical networks

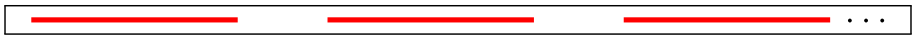

Fig. 2 Red lines denote the active time of neurons in day, while the gap shows the inactive time of neurons at night (color figure online)

with delays on time scales were studied by employing the Lyapunov–Krasovskii functional and unified Jensen's inequalities. The works in Wang et al. [54] investigated the problem of synchronization of non-autonomous recurrent neural networks with delays on time scales by applying the comparison lemma and Lyapunov techniques. In Huang et al. [55], the authors studied quasi-synchronization results for neural networks with parameter mismatches on time scales using the Lyapunov functional method. Recently, Kumar et al. [56] investigated the exponential lag synchronization results of Cohen–Grossberg-type neural networks with mixed delays on time scales by using the matrix-measure and Halanay inequality. It should be noted that the synchronization results for continuous and discrete systems with parameter mismatches have been studied in [28–30, 32, 34–36, 38], with some utilizing the Lyapunov method [28, 32, 36] and others employing the matrix-measure method [29, 30, 34, 35, 38]. However, these results cannot be easily applied and extended to the hybrid time domains. Also, to the best of the authors' knowledge, there is no work reported on the projective lag quasi-synchronization (PLQS) of coupled dynamic systems on hybrid-type time domains.

When it comes to considering coupled systems on time scales, several relevant questions arise, such as: What type of time scales conditions must be met for different types of synchronization? Does any relationship exist between synchronization and time scale? It is well known that for computational purposes, continuous-time systems described by differential equations are discretized, in such cases, how can one ensure the selection of an appropriate discrete-time system? Can the synchronization error bound in the existing literature be further refined? Motivated by the above discussion and questions, this manuscript aims to establish PLQS results for coupled dynamic systems with mixed delays and parameter mismatches on time scales using the matrix-measure technique. The main contributions of this manuscript can be highlighted as follows.

- We apply the time scales approach to investigate the problem of PLQS for coupled dynamic systems on arbitrary time domains with mixed delays and parameter mismatches.
- Continuous and discrete-time domains are the particular cases of time scales, and hence, the obtained PLQS scheme is not just true for the continuous-time or discrete-time state analysis, but additionally hold for any mixture of these two, which provides a wider range of applications.
- We refine the theoretical error bound so that it is close to the simulation error.
- We also provide conditions under which the obtained results can be extended to the case of projective quasi-synchronization, lag quasi-synchronization, and quasi-synchronization.
- Three examples are presented to validate the analytical outcomes of this manuscript.

The rest of the manuscript is structured as follows: We provide fundamental notations, definitions, and lemmas in Sect. 2. Section 3 presents the statement of the proposed problem. We establish the main results of this manuscript in Sect. 4. Finally, in Sect. 5, we provide three illustrative examples to validate the obtained analytical results.

2 Preliminaries

We use Id to represent the identity matrix of suitable order and superscript T for matrix transpose. The symbol $\emptyset$ denotes the empty set. The space $\mathbb{R}^n$ refers to the n-dimensional Euclidean space. The collection of all continuous functions from $[a,b]_{\mathbb{T}}$ into $\mathbb{R}^n$, represented by $C([a,b]_{\mathbb{T}},\mathbb{R}^n)$, form a Banach space equipped with the induced norm $\|x\|_p = \sup_{t\in[a,b]_{\mathbb{T}}} \|x(t)\|_p$, where $p \in \{1,2,\infty\}$ and $\|\cdot\|_p$ is a vector norm. For any $x \in \mathbb{R}^n$ and $p = 1,2,\infty$, the vector norm is defined as

$$\|x\|_1 = \sum_{k=1}^{n} |x_k|,\ \|x\|_2 = \sqrt{\sum_{k=1}^{n} x_k^2},\ \|x\|_\infty = \max_{1\le k\le n} |x_k|.$$

Next, we recall some basic definitions of time scales and matrix-measure which will be used in the subsequent sections.

A *time scale* is a non-empty closed subset of the real numbers $\mathbb{R}$ which inherits its topology and ordering from $\mathbb{R}$. Now onwards, we denote a time scale by $\mathbb{T}$. $\mathbb{R}$, $h\mathbb{Z}$ for $h > 0$, and $\mathbb{P}_{c,d} = \bigcup_{l=0}^{\infty}[l(c+d), l(c+d)+d], c, d \in \mathbb{R}^+$ are some typical examples of time scales. We represent a time scale interval as $[c,d]_{\mathbb{T}}$, which is defined as the set $t \in \mathbb{T} : c \le t \le d$.

The *backward* and *forward jump operators* $\rho, \sigma : \mathbb{T} \to \mathbb{T}$ are defined as $\rho(t) = \sup\{r < t : r \in \mathbb{T}\}$ and $\sigma(t) = \inf\{r > t : r \in \mathbb{T}\}$, respectively, with the substitutions $\sup\emptyset = \inf\mathbb{T}$ and $\inf\emptyset = \sup\mathbb{T}$. Additionally, we define the *graininess* function $\mu : \mathbb{T} \to [0,\infty)$ as $\mu(t) = \sigma(t) - t$. For $t \in \mathbb{T}$, if $t < \sup\mathbb{T}$ and $\sigma(t) = t$, then t is called right-dense point of $\mathbb{T}$.

Let us define the set $\mathbb{T}^\kappa$ as follows:

$$\mathbb{T}^{\kappa} = \begin{cases} \mathbb{T}^{\kappa} \setminus (\rho(\sup(\mathbb{T})), \sup(\mathbb{T})] & \text{if } \sup \mathbb{T} < \infty, \\ \mathbb{T} & \text{if } \sup \mathbb{T} = \infty. \end{cases}$$

Now, we will provide the definition of the delta derivative (also known as the Hilger derivative), which extends the notions of the ordinary derivative and difference operator.

Definition 1 ([54], Def. 1) Let $f : \mathbb{T} \to \mathbb{R}$ be a function and $t \in \mathbb{T}^{\kappa}$. The *Hilger (or delta) derivative* of f at t, denoted by $f^{\Delta}(t)$, is defined as the number (if it exists) such that for any given $\epsilon > 0$, there exists a neighbourhood U of t satisfying the inequality

$$|[f(\sigma(t)) - f(s)] - f^{\Delta}(t)[\sigma(t) - s]| \leq \epsilon |\sigma(t) - s|$$

for all $s \in U$. Furthermore, the delta derivative can be referred to as the *upper right Dini- Δ-derivative* denoted by $D^{+}_{\Delta} f(t)$, if the right-sided neighbourhood U^{+} replaces the neighbourhood U.

Remark 1 In Definition 1, if we consider

- $\mathbb{T} = h\mathbb{Z}$, $h > 0$, then the delta derivative $f^{\Delta}(t)$ becomes the usual h-difference forward operator, i.e. $f^{\Delta}(t) = \Delta^{h} f(t) = \frac{f(t+h)-f(t)}{h}$.
- $\mathbb{T} = \mathbb{R}$, then the delta derivative $f^{\Delta}(t)$ becomes the usual ordinary derivative $f'(t)$ and the upper right Dini-Δ-derivative $D^{+}_{\Delta} f(t)$ becomes the ordinary upper right Dini-derivative $D^{+} f(t)$.

Theorem 1 ([39], *Theorem* 1.16) Assume that $f : \mathbb{T} \to \mathbb{R}$ is differentiable at $t \in \mathbb{T}^{\kappa}$, then we have

$$f(\sigma(t)) = f(t) + \mu(t) f^{\Delta}(t).$$

A function $f : \mathbb{T} \to \mathbb{R}$ is said to be *regressive* (or *positive regressive*) if $1 + \mu(t) f(t) \neq 0$ (or > 0) for all $t \in \mathbb{T}$. Further, f is said to be a *regulated* function if its right and left side limit exists (finitely) at all right and left dense points of $\mathbb{T}$, respectively. Additionally, a regulated function f is said to be *rd-continuous*, if it is continuous at all the right-dense points of $\mathbb{T}$. The sets of all rd-continuous functions and rd-continuous regressive (positive) functions on $\mathbb{T}$ are denoted by $C_{rd}(\mathbb{T}, \mathbb{R})$ and $\mathcal{R}(\mathcal{R}^{+})$, respectively.

The generalized delta integral on time scales is defined as follows.

Definition 2 ([39], Def. 1.71) A function $F : \mathbb{T} \to \mathbb{R}$ is said to be an *anti-derivative* of a regulated function $f : \mathbb{T} \to \mathbb{R}$, if for all $t \in \mathbb{T}^{\kappa}$, the relation $F^{\Delta}(t) = f(t)$ holds. Further, the Cauchy integral is defined by

$$\int_{c}^{d} f(s)\Delta s = F(d) - F(c) \quad \text{for all } c, d \in \mathbb{T}.$$

Theorem 2 ([39], *Theorem.* 1.77) Let $c, d \in \mathbb{T}$ and $f \in C_{rd}(\mathbb{T}, \mathbb{R})$, then, for

- $\mathbb{T} = h\mathbb{Z} = \{hk : k \in \mathbb{Z}\}$, where $h > 0$, we have

$$\int_{c}^{d} f(s)\Delta s = \begin{cases} \sum_{k=\frac{c}{h}}^{\frac{d}{h}-1} h f(kh) & \text{if } c < d, \\ 0 & \text{if } c = d, \\ -\sum_{k=\frac{d}{h}}^{\frac{c}{h}-1} h f(kh) & \text{if } c > d. \end{cases}$$

- $\mathbb{T} = \mathbb{R}$, we have

$$\int_{c}^{d} f(s)\Delta s = \int_{c}^{d} f(s) ds.$$

In the next definition, we are defining the classical matrix-measure.

Definition 3 ([57], Def. 2.1) For a real square matrix $A = (a_{kl})_{n\times n}$, the *classical matrix-measure* with respect to the $p-$norm ($p = 1, 2$ or ∞) is defined as

$$\Upsilon_{p}(A) = \lim_{s \to 0^{+}} \frac{\| \mathrm{Id} + sA \|_{p} - 1}{s},$$

where $\| \cdot \|_{p}$ is the induced matrix norm on $\mathbb{R}^{n\times n}$. Table 1 provides the matrix norms and related measures.

Next, we recall how the matrix-measure is generalized to time scales:

Definition 4 ([48], Def. 2) For a real square matrix $A = (a_{kl})_{n\times n}$, the *unified matrix-measure* on an arbitrary time scale $\mathbb{T}$ with respect to the $p-$norm ($p = 1, 2$ or ∞) is defined as

$$M_{p}(A, \mathbb{T}) = \begin{cases} \max\left\{ \frac{\| \mathrm{Id} + \mu(t)A \|_{p} - 1}{\mu(t)} : t \in \mathbb{T} \right\}, \text{if } \mu(t) > 0, \forall\, t \in \mathbb{T}, \\ \max\left\{ \Upsilon_{p}(A),\ \max\left\{ \frac{\| \mathrm{Id} + \mu(t)A \|_{p} - 1}{\mu(t)} :\ t \in \mathbb{T}, \mu(t) > 0 \right\} \right\}, \text{ else.} \end{cases}$$

Table 1 Matrix norms and related measures

Matrix norm	Matrix-measure
$\|A\|_{1} = \max_{j} \sum_{i=1}^{n} \|a_{ij}\|$	$\Upsilon_{1}(A) = \max_{j} a_{jj} + \sum_{i=1, i\neq j}^{n} \|a_{ij}\|$
$\|A\|_{2} = \sqrt{\lambda_{\max}(A^{T}A)}$	$\Upsilon_{2}(A) = \frac{1}{2}\lambda_{\max}(A^{T} + A)$
$\|A\|_{\infty} = \max_{i} \sum_{j=1}^{n} \|a_{ij}\|$	$\Upsilon_{\infty}(A) = \max_{i} a_{ii} + \sum_{j=1, \neq i}^{n} \|a_{ij}\|$

Note that for $\mathbb{T} = \mathbb{R}$, Definition 4 reduces to Definition 3. Also, for $\mathbb{T} = h\mathbb{Z}$, $h > 0$, which means that $\mu(t) = h$ for all $t \in \mathbb{T}$, Definition 4 reads

$$\omega_p(A, h) = \frac{\|\operatorname{Id} + hA\|_p - 1}{h}.$$

We are ending this section by giving the following important result:

Theorem 3 (*Halanay inequality* [41], *Theorem* 2.1) Let $z(t) \in C_{rd}(\mathbb{T}, \mathbb{R})$ be a nonnegative function satisfying

$$\begin{cases} D_{\Delta}^{+} z(t) & \leq -a(t)z(t) + b(t)\sup_{s\in[t-\vartheta,t]_{\mathbb{T}}} z(s) + c(t),\ t \in [0,\infty)_{\mathbb{T}}, \\ z(s) & = \Phi(s),\ s \in [-\vartheta, 0]_{\mathbb{T}}, \end{cases}$$

where $\vartheta > 0, a(t), b(t), c(t)$ are nonnegative rd-continuous functions, $\Phi \in C_{rd}([-\vartheta, 0]_{\mathbb{T}}, \mathbb{R})$, and $-a(t) \in \mathcal{R}^{+}$. If there exist constants $\delta > 0$ and $k \in (0, 1)$ such that

$$a(t) - b(t) \geq \delta > 0, \quad ka(t) - b(t) > 0,\ t \in [0,\infty)_{\mathbb{T}},$$

then for any given $\epsilon > 0$, there exists a $T = T(M, \epsilon) > 0$ such that

$$z(t) \leq \frac{c}{\delta} + \epsilon,\ t \in [T,\infty)_{\mathbb{T}},$$

where $c = \sup_{t\geq -\vartheta} c(t)$ and $M = \sup_{s\in[-\vartheta,0]_{\mathbb{T}}} |\Phi(s)|$.

3 Problem description

We consider the following coupled dynamical system with discrete and distributed delays on time scales:

$$\begin{cases} x^{\Delta}(t) = \widehat{\mathcal{Q}}x(t) + \widehat{\mathcal{R}}\mathcal{F}(x(t)) \\ \qquad\quad +\widehat{\mathcal{S}}\mathcal{G}(x(t-\vartheta_1(t))) + \widehat{\mathcal{T}}\int_{t-\vartheta_2(t)}^{t}\mathcal{H}(x(s))\Delta s,\ t \in [0,\infty)_{\mathbb{T}}, \\ x(s) = \hat{\phi}(s),\ s \in [-\vartheta, 0]_{\mathbb{T}}, \end{cases} \tag{1}$$

where $x(t) \in \mathbb{R}^n$; $\hat{\mathcal{Q}}, \hat{\mathcal{R}}, \hat{\mathcal{S}}, \hat{\mathcal{T}} \in \mathbb{R}^{n\times n}$ are constant matrices; $\vartheta_1(t)(>0)$ is the discrete delay such that $t - \vartheta_1(t) \in \mathbb{T}$ and $0 \leq \vartheta_1(t) \leq \eta_1$ for all $t \in \mathbb{T}$; $\vartheta_2(t)(>0)$ is the distributed delay such that $t - \vartheta_2(t) \in \mathbb{T}$ and $0 \leq \vartheta_2(t) \leq \eta_2$ for all $t \in \mathbb{T}$; η_1 and η_2 are positive constants; $\eta = \max\{\eta_1, \eta_2\}$; $\hat{\phi} \in C_{rd}([-\eta, 0]_{\mathbb{T}}, \mathbb{R}^n)$; and $\mathcal{F}(x(\cdot)), \mathcal{G}(x(\cdot)), \mathcal{H}(x(\cdot))$ are functions in $\mathbb{R}^n$ which satisfy certain conditions to be specified later.

Let us consider the system (1) as the drive system and the corresponding response system with parameter mismatches in the coefficient matrices as

$$\begin{cases} y^{\Delta}(t) = \mathcal{Q}y(t) + \mathcal{R}\mathcal{F}(y(t)) + \mathcal{S}\mathcal{G}(y(t-\vartheta_1(t))) \\ \qquad\quad +\mathcal{T}\int_{t-\vartheta_2(t)}^{t}\mathcal{H}(y(s))\Delta s + u(t),\ t \in [0,\infty)_{\mathbb{T}}, \\ y(s) = \phi(s),\ s \in [-\eta, 0]_{\mathbb{T}}, \end{cases} \tag{2}$$

where $y(t) \in \mathbb{R}^n$; $\mathcal{Q}, \mathcal{R}, \mathcal{S}, \mathcal{T} \in \mathbb{R}^{n\times n}$ are constant matrices such that $\hat{\mathcal{Q}} \neq \mathcal{Q}, \hat{\mathcal{R}} \neq \mathcal{R}, \hat{\mathcal{S}} \neq \mathcal{S}, \hat{\mathcal{T}} \neq \mathcal{T}$; $\phi \in C_{rd}([-\eta, 0]_{\mathbb{T}}, \mathbb{R}^n)$. Due to the finite speed of transmission and spreading, there is a time delay associated with the signal travelling from the master system to the slave system. To account for this delay, we introduce the following controller

$$u(t) = -\mathcal{K}(y(t) - \alpha x(t-\varsigma)), \tag{3}$$

where $\mathcal{K}$ is the coupling matrix, α is the projective constant, and ς is the transmittal delay with $t - \varsigma \in \mathbb{T}$.

Let's define the error by $e(t) = y(t) - \alpha x(t-\varsigma)$, between the drive system (1) and the response system (2), so that the related error dynamical system can be written as

$$\begin{aligned} e^{\Delta}(t) = {} & (\mathcal{Q} - \mathcal{K})e(t) + \mathcal{R}\bar{\mathcal{F}}(e(t)) + \mathcal{S}\bar{\mathcal{G}}(e(t-\vartheta_1(t))) \\ & + \mathcal{T}\int_{t-\vartheta_2(t)}^{t}\bar{\mathcal{H}}(e(s))\Delta s \\ & + F(x, \vartheta_1(t), \vartheta_2(t), \alpha, \varsigma), \end{aligned} \tag{4}$$

where $e(t) \in \mathbb{R}^n$; $\bar{\mathcal{F}}(e(\cdot)) := \mathcal{F}(y(\cdot)) - \mathcal{F}(y(\cdot) - e(\cdot))$; $\bar{\mathcal{G}}(e(\cdot)) := \mathcal{G}(y(\cdot)) - \mathcal{G}(y(\cdot) - e(\cdot))$; $\bar{\mathcal{H}}(e(\cdot)) := \mathcal{H}(y(\cdot)) - \mathcal{H}(y(\cdot) - e(\cdot))$ and

$$\begin{aligned} & F(x, \vartheta_1(t), \vartheta_2(t), \alpha, \varsigma) \\ & := \alpha(\mathcal{Q} - \hat{\mathcal{Q}})x(t-\varsigma) + \mathcal{R}\mathcal{F}(\alpha x(t-\varsigma)) - \alpha\hat{\mathcal{R}}\mathcal{F}(x(t-\varsigma)) \\ & \quad + \mathcal{S}\mathcal{G}(\alpha x(t-\varsigma-\vartheta_1(t))) - \alpha\hat{\mathcal{S}}\mathcal{G}(x(t-\varsigma-\vartheta_1(t))) \\ & \quad + \int_{t-\vartheta_2(t)}^{t}(\mathcal{T}\mathcal{H}(\alpha x(s-\varsigma)) - \alpha\hat{\mathcal{T}}\mathcal{H}(x(s-\varsigma)))\Delta s. \end{aligned}$$

To account for the delays, we set $x(s) = \hat{\phi}(-\eta)$ for all $s \in [-\eta - \varsigma, -\eta]_{\mathbb{T}}$ and

$$\psi(s) = \begin{cases} \hat{\phi}(s),\ s \in [-\eta, 0]_{\mathbb{T}}, \\ \hat{\phi}(-\eta),\ s \in [-\eta - \varsigma, -\eta]_{\mathbb{T}}. \end{cases}$$

The initial condition for the error dynamics (4) can be defined by

$$e(s) = \phi(s) - \psi(s-\varsigma),\ s \in [-\eta, 0]_{\mathbb{T}}.$$

It could be noticed that, due to the parameter mismatches between the drive systems (1) and response system (2), the origin $e = 0$ is not an equilibrium point of the error system (4); therefore, complete projective lag synchronization is not possible. However, we provide the PLQS scheme which synchronizes the drive-response systems up

to a small error bound. Mathematically we can define the PLQS as follows.

Definition 5 The drive system (1) and the response system (2) are said to be *projective lag quasi-synchronized* to an error bound ϵ_p in the timescale sense if it holds that

$$\|y(t) - \alpha x(t-\varsigma)\|_p \le \epsilon_p \text{ as } t \to \infty.$$

Remark 2 In Definition 5, the drive system (1) and the response system (2) are called

- *projective quasi-synchronized* to the error bound ϵ_p, if $\varsigma = 0$;
- *lag quasi-synchronized* to the error bound ϵ_p, if $\alpha = 1$;
- *quasi-synchronized* to the error bound ϵ_p, if $\alpha = 1$ and $\varsigma = 0$.

To prove the main results, we need the following assumptions.

Assumption 1 (Ass. 3 in [34]) The state x of the drive system evolves in a bounded state space $\Omega \subset \mathbb{R}^n$. In particular, there exists a constant β_p so that $\|x(t)\|_p \le \beta_p$ for $p = 1, 2, \infty$.

Assumption 2 (Ass. 1 in [34]) $\mathcal{F}, \mathcal{G}$, and $\mathcal{H}$ are Lipschitz on Ω, i.e. for any $z_1, z_2 \in \Omega$, there exist positive constants $L_\mathcal{F}, L_\mathcal{G}$, and $L_\mathcal{H}$ such that

$$\begin{aligned}
\|\mathcal{F}(z_1) - \mathcal{F}(z_2)\|_p &\le L_\mathcal{F}\|z_1 - z_2\|_p,\\
\|\mathcal{G}(z_1) - \mathcal{G}(z_2)\|_p &\le L_\mathcal{G}\|z_1 - z_2\|_p,\\
\|\mathcal{H}(z_1) - \mathcal{H}(z_2)\|_p &\le L_\mathcal{H}\|z_1 - z_2\|_p
\end{aligned}$$

for $p = 1, 2, \infty$.

Remark 3 Note that in many applied neural networks, typical choices of the activation functions like *tanh* or *Sigmoid* fulfil Assumption 2. Moreover, in Assumption 2, we do not require $f(0) = 0$ and $g(0) = 0$ which is required in some existing works [29, 34]. This implies that a broad spectrum of nonlinear functions satisfies Assumption 2.

Remark 4 In the previous studies [5, 6], time delays have been considered as differentiable, but in this study, we do not require such assumption.

Remark 5 Since $\mathcal{F}, \mathcal{G}$, and $\mathcal{H}$ are Lipschitz on Ω, they are also bounded on Ω. This means that there exist positive constants $K_\mathcal{F}, K_\mathcal{G}$, and $K_\mathcal{H}$ such that $\|\mathcal{F}(z)\|_p \le K_\mathcal{F}$, $\|\mathcal{G}(z)\|_p \le K_\mathcal{G}$, and $\|\mathcal{H}(z)\|_p \le K_\mathcal{H}$ for all $z \in \Omega$ and $p = 1, 2, \infty$.

4 Projective lag quasi-synchronization

In this section, we will derive some sufficient conditions for PLQS of the drive system (1) and the response system (2) by using the matrix-measure theory and generalized Halanay inequality. Prior to that, we introduce an important lemma that is required to establish these conditions.

Lemma 1 *Under Assumptions 1 and 2, $F(x, \vartheta_1(t), \vartheta_2(t), \alpha, \varsigma)$ is bounded by a constant $c_p > 0$, i.e.* $\|F(x, \vartheta_1(t), \vartheta_2(t), \alpha, \varsigma)\|_p \le c_p$,

where

$$\begin{aligned}
c_p = {} & |\alpha|\|(\mathcal{Q} - \hat{\mathcal{Q}})\|_p\beta_p + (\|\mathcal{R}\|_p + |\alpha|\|\hat{\mathcal{R}}\|_p)K_\mathcal{F}\\
& + (\|\mathcal{S}\|_p + |\alpha|\|\hat{\mathcal{S}}\|_p)K_\mathcal{G}\\
& + \eta_2(\|\mathcal{T}\|_p + |\alpha|\|\hat{\mathcal{T}}\|_p)K_\mathcal{H}.
\end{aligned}$$

Proof For any $x \in \Omega$, we have

$$\begin{aligned}
&\|F(x, \vartheta_1(t), \vartheta_2(t), \alpha, \varsigma)\|_p\\
&\le \|\alpha(\mathcal{Q} - \hat{\mathcal{Q}})x(t-\varsigma)\|_p + \|\mathcal{R}\mathcal{F}(\alpha x(t-\varsigma)) - \alpha\hat{\mathcal{R}}\mathcal{F}(x(t-\varsigma))\|_p\\
&\quad + \|\mathcal{S}\mathcal{G}(\alpha x(t-\varsigma-\vartheta_1(t))) - \alpha\hat{\mathcal{S}}\mathcal{G}(x(t-\varsigma-\vartheta_1(t)))\|_p\\
&\quad + \|\int_{t-\vartheta_2(t)}^{t}(\mathcal{T}\mathcal{H}(\alpha x(s-\varsigma)) - \alpha\hat{\mathcal{T}}\mathcal{H}(x(s-\varsigma)))\Delta s\|_p.
\end{aligned} \tag{5}$$

Now, from Assumptions 1 and 2, we get

$$\begin{aligned}
&\|\mathcal{R}\mathcal{F}(\alpha x(t-\varsigma)) - \alpha\hat{\mathcal{R}}\mathcal{F}(x(t-\varsigma))\|_p\\
&\quad \le \|\mathcal{R}\mathcal{F}(\alpha x(t-\varsigma))\|_p + \|\alpha\hat{\mathcal{R}}\mathcal{F}(x(t-\varsigma))\|_p\\
&\quad \le \|\mathcal{R}\|_p K_\mathcal{F} + |\alpha|\|\hat{\mathcal{R}}\|_p K_\mathcal{F}.
\end{aligned} \tag{6}$$

Similarly, we obtain

$$\begin{aligned}
&\|\mathcal{S}\mathcal{G}(\alpha x(t-\varsigma-\vartheta_1(t))) - \alpha\hat{\mathcal{S}}\mathcal{G}(x(t-\varsigma-\vartheta_1(t)))\|_p\\
&\quad \le \|\mathcal{S}\|_p K_\mathcal{G} + |\alpha|\|\hat{\mathcal{S}}\|_p K_\mathcal{G}
\end{aligned} \tag{7}$$

and

$$\begin{aligned}
&\int_{t-\vartheta_2(t)}^{t}(\|\mathcal{T}\mathcal{H}(\alpha x(s-\varsigma)) - \alpha\hat{\mathcal{T}}\mathcal{H}(x(t-\varsigma))\|_p)\Delta s\\
&\quad \le \eta_2\|\mathcal{T}\|_p K_\mathcal{H} + \eta_2|\alpha|\|\hat{\mathcal{T}}\|_p K_\mathcal{H}.
\end{aligned} \tag{8}$$

Therefore, from the equations (5), (6), (7) and (8), we get

$$\begin{aligned}
&\|F(x, \vartheta_1(t), \vartheta_2(t), \alpha, \varsigma)\|_p\\
&\quad \le |\alpha|\|(\mathcal{Q} - \hat{\mathcal{Q}})\|_p\beta_p + (\|\mathcal{R}\|_p + |\alpha|\|\hat{\mathcal{R}}\|_p)K_\mathcal{F} + (\|\mathcal{S}\|_p\\
&\quad + |\alpha|\|\hat{\mathcal{S}}\|_p)K_\mathcal{G} + \eta_2(\|\mathcal{T}\|_p + |\alpha|\|\hat{\mathcal{T}}\|_p)K_\mathcal{H}\\
&\quad = c_p,
\end{aligned}$$

where $c_p > 0$ is a constant. □

Remark 6 In Lemma 1, if $\alpha = 1$, then the constant c_p can be calculated as

$$c_p = \|(\mathcal{Q} - \hat{\mathcal{Q}})\|_p \beta_p + (\|\mathcal{R}\|_p - \|\hat{\mathcal{R}}\|_p) K_{\mathcal{F}} + (\|\mathcal{S}\|_p - \|\hat{\mathcal{S}}\|_p) K_{\mathcal{G}} + \eta_2 (\|\mathcal{T}\|_p - \|\hat{\mathcal{T}}\|_p) K_{\mathcal{H}}.$$

Now, we are in a position to give the first main result of PLQS for the drive system (1) and response system (2) as follows.

Theorem 4 *Let Assumptions 1 and 2 hold, then the drive system (1) and the response system (2) are projective lag quasi-synchronized with an error level*

$$\epsilon_p = \frac{\|\mathcal{B}^{-1}\|_p \|\mathcal{B}\|_p c_p}{\delta_p},$$

if, for some $p \in \{1, 2, \infty\}$, there exist a non-singular matrix $\mathcal{B}$, a coupling matrix $\mathcal{K}$, and a constant $k \in (0, 1)$ such that

$$\mathcal{M}_{(1,p)} - \mathcal{M}_{(2,p)} \geq \delta_p > 0, \; k\mathcal{M}_{(1,p)} - \mathcal{M}_{(2,p)} > 0$$

and $-\mathcal{M}_{(1,p)} \in \mathcal{R}^+$, where

$$\mathcal{M}_{(1,p)} = -(M_p(\mathcal{B}(\mathcal{Q} - \mathcal{K})\mathcal{B}^{-1}, \mathbb{T}) + L_{\mathcal{F}} \|\mathcal{B}\|_p \|\mathcal{R}\|_p \|\mathcal{B}^{-1}\|_p),$$
$$\mathcal{M}_{(2,p)} = L_{\mathcal{G}} \|\mathcal{B}\|_p \|\mathcal{S}\|_p \|\mathcal{B}^{-1}\|_p + \eta_2 L_{\mathcal{H}} \|\mathcal{B}\|_p \|\mathcal{T}\|_p \|\mathcal{B}^{-1}\|_p$$

and c_p is the same as defined in Lemma 1.

Proof Let us define

$$V(t) = \|\mathcal{B}e(t)\|_p.$$

For any point $t \in \mathbb{T}$, there are two possibilities: either $\mu(t) = 0$ or $\mu(t) > 0$. As a result, we separate the proof into two cases as follows:

Case 1: When $\mu(t) > 0$, then we have

$$\begin{aligned}
&\frac{\|\mathcal{B}e(\sigma(t))\|_p - \|\mathcal{B}e(t)\|_p}{\mu(t)} \\
&= \frac{1}{\mu(t)} \Big\{ \|\mathcal{B}e(t) + \mu(t)\mathcal{B}e^{\Delta}(t)\|_p - \|\mathcal{B}e(t)\|_p \Big\} \\
&= \frac{1}{\mu(t)} \Big\{ \|\mathcal{B}e(t) + \mu(t)\mathcal{B}((\mathcal{Q} - \mathcal{K})e(t) + \mathcal{R}\bar{\mathcal{F}}(e(t)) \\
&\quad + \mathcal{S}\bar{\mathcal{G}}(e(t - \vartheta_1(t))) + \mathcal{T} \int_{t-\vartheta_2(t)}^{t} \bar{\mathcal{H}}(e(s))\Delta s \\
&\quad + F(x, \vartheta_1(t), \vartheta_2(t), \alpha, \varsigma)\|_p - \|\mathcal{B}e(t)\|_p \Big\} \\
&\leq \frac{1}{\mu(t)} \Big\{ \|\mathcal{B}e(t) + \mu(t)\mathcal{B}(\mathcal{Q} - \mathcal{K})e(t)\|_p - \|\mathcal{B}e(t)\|_p \Big\} \\
&\quad + \|\mathcal{B}\mathcal{S}\bar{\mathcal{G}}(e(t - \vartheta_1(t)))\|_p + \|\mathcal{B}\mathcal{T} \int_{t-\vartheta_2(t)}^{t} \mathcal{H}(e(s))\Delta s\|_p \\
&\quad + \|\mathcal{B}\mathcal{R}\bar{\mathcal{F}}(e(t))\|_p + \|\mathcal{B}F(x, \vartheta_1(t), \vartheta_2(t), \alpha, \varsigma)\|_p.
\end{aligned} \tag{9}$$

Now, from Assumption 2, we have

$$\begin{aligned}
\|\bar{\mathcal{F}}(e(t))\|_p &= \|\mathcal{F}(y(t)) - \mathcal{F}(y(t) - e(t))\|_p \\
&\leq L_{\mathcal{F}} \|y(t) - \alpha x(t - \varsigma)\|_p = L_{\mathcal{F}} \|e(t)\|_p.
\end{aligned} \tag{10}$$

Similarly, we obtain

$$\|\bar{\mathcal{G}}(e(t - \vartheta_1(t)))\|_p \leq L_{\mathcal{G}} \|e(t - \vartheta_1(t))\|_p \tag{11}$$

and

$$\|\bar{\mathcal{H}}(e(t))\|_p \leq L_{\mathcal{H}} \|e(t)\|_p. \tag{12}$$

Now, from the inequalities (9), (10), (11), (12) and Lemma 1, we obtain

$$\begin{aligned}
&\frac{\|\mathcal{B}e(\sigma(t))\|_p - \|\mathcal{B}e(t)\|_p}{\mu(t)} \\
&\leq \frac{\|\operatorname{Id} + \mu(t)\mathcal{B}(\mathcal{Q} - \mathcal{K})\mathcal{B}^{-1}\|_p - 1}{\mu(t)} \|\mathcal{B}e(t)\|_p \\
&\quad + L_{\mathcal{F}} \|\mathcal{B}\|_p \|\mathcal{R}\|_p \|\mathcal{B}^{-1}\|_p \|\mathcal{B}e(t)\|_p \\
&\quad + L_{\mathcal{G}} \|\mathcal{B}\|_p \|\mathcal{S}\|_p \|\mathcal{B}^{-1}\|_p \|\mathcal{B}e(t - \vartheta_1(t))\|_p \\
&\quad + \eta_2 L_{\mathcal{H}} \|\mathcal{B}\|_p \|\mathcal{T}\|_p \|\mathcal{B}^{-1}\|_p \sup_{s \in [t-\eta_2, t]} \|\mathcal{B}e(s)\|_p + \|\mathcal{B}\|_p c_p \\
&\leq (M_p(\mathcal{B}(\mathcal{Q} - \mathcal{K})\mathcal{B}^{-1}, \mathbb{T}) + L_{\mathcal{F}} \|\mathcal{B}\|_p \|\mathcal{R}\|_p \|\mathcal{B}^{-1}\|_p) \|\mathcal{B}e(t)\|_p \\
&\quad + \|\mathcal{B}\|_p c_p + (L_{\mathcal{G}} \|\mathcal{B}\|_p \|\mathcal{S}\|_p \|\mathcal{B}^{-1}\|_p \\
&\quad + \eta_2 L_{\mathcal{H}} \|\mathcal{B}\|_p \|\mathcal{T}\|_p \|\mathcal{B}^{-1}\|_p) \sup_{s \in [t-\eta, t]} \|\mathcal{B}e(s)\|_p \\
&\leq -\mathcal{M}_{(1,p)} \|\mathcal{B}e(t)\|_p + \mathcal{M}_{(2,p)} \sup_{s \in [t-\eta, t]_{\mathbb{T}}} \|\mathcal{B}e(s)\|_p + \|\mathcal{B}\|_p c_p.
\end{aligned}$$

Hence, using Definition 1, we obtain

$$\begin{aligned}
D_{\Delta}^{+} V(t) \leq &-\mathcal{M}_{(1,p)} V(t) + \mathcal{M}_{(2,p)} \sup_{s \in [t-\eta, t]_{\mathbb{T}}} V(s) \\
&+ \|\mathcal{B}\|_p c_p.
\end{aligned} \tag{13}$$

Case 2: When $\mu(t) = 0$, the delta derivative becomes the ordinary derivative, i.e. $z^{\Delta}(t) = z'(t)$. Accordingly, by applying the formula $z(t + h) = z(t) + z'(t)h + \mathrm{r}_z(h)$ with $\lim_{h \to 0} \frac{\|\mathrm{r}_z(h)\|_p}{h} = 0$, we obtain

$$
\begin{aligned}
&\lim_{h\to 0^+}\frac{\|\mathcal{B}e(t+h)\|_p-\|\mathcal{B}e(t)\|_p}{h}\\
&=\lim_{h\to 0^+}\frac{1}{h}\Big\{\|\mathcal{B}e(t)+h\mathcal{B}e^{\Delta}(t)+\mathrm{r}_e(h)\|_p-\|\mathcal{B}e(t)\|_p\Big\}\\
&\le\lim_{h\to 0^+}\frac{1}{h}\Big\{\|\mathcal{B}e(t)+h\mathcal{B}((\mathcal{Q}-\mathcal{K})e(t)+\mathcal{R}\bar{\mathcal{F}}(e(t))\\
&\quad+\mathcal{S}\bar{\mathcal{G}}(e(t-\vartheta_1(t)))+\mathcal{T}\int_{t-\vartheta_2(t)}^{t}\bar{\mathcal{H}}(e(s))\Delta s\\
&\quad+F(x,\vartheta_1(t),\vartheta_2(t),\alpha,\varsigma)+\mathrm{r}_e(h)\|_p-\|\mathcal{B}e(t)\|_p\Big\}\\
&\le(M_p(\mathcal{B}(\mathcal{Q}-\mathcal{K})\mathcal{B}^{-1},\mathbb{T})+L_{\mathcal{F}}\|\mathcal{B}\|_p\|\mathcal{R}\|_p\|\mathcal{B}^{-1}\|_p)\|\mathcal{B}e(t)\|_p\\
&\quad+\|\mathcal{B}\|_p c_p+(L_{\mathcal{G}}\|\mathcal{B}\|_p\|\mathcal{S}\|_p\|\mathcal{B}^{-1}\|_p\\
&\quad+\eta_2 L_{\mathcal{H}}\|\mathcal{B}\|_p\|\mathcal{T}\|_p\|\mathcal{B}^{-1}\|_p)\sup_{s\in[t-\eta,t]}\|\mathcal{B}e(s)\|_p\\
&\le-\mathcal{M}_{(1,p)}\|\mathcal{B}e(t)\|_p+\mathcal{M}_{(2,p)}\sup_{s\in[t-\eta,t]_{\mathbb{T}}}\\
&\quad\|\mathcal{B}e(s)\|_p+\|\mathcal{B}\|_p c_p.
\end{aligned}
$$

Therefore, by utilizing Definition 1, we obtain the same inequality as (13).

As a result of the above two cases, for each $t\in\mathbb{T}$, we obtain

$$
D_{\Delta}^{+}V(t)\le-\mathcal{M}_{(1,p)}V(t)+\mathcal{M}_{(2,p)}\sup_{s\in[t-\eta,t]_{\mathbb{T}}}V(s)+\|\mathcal{B}\|_p c_p.
$$

Therefore, from Lemma 3, we get

$$
V(t)\le\frac{\|\mathcal{B}\|_p c_p}{\delta_p}+\epsilon.
$$

Subsequently, we obtain

$$
\begin{aligned}
\|e(t)\|_p&=\|\mathcal{B}^{-1}\mathcal{B}e(t)\|_p\\
&\le\|\mathcal{B}^{-1}\|_p\|V(e(t))\|_p\\
&\le\frac{\|\mathcal{B}^{-1}\|_p\|\mathcal{B}\|_p c_p}{\delta_p}+\|\mathcal{B}^{-1}\|_p\|\mathcal{B}\|_p\epsilon.
\end{aligned}
$$

Hence, the drive system (1) and the response system (2) are projective lag quasi-synchronized to the error level $\epsilon_p=\frac{\|\mathcal{B}^{-1}\|_p\|\mathcal{B}\|_p c_p}{\delta_p}$. □

Remark 7 The error bound level ϵ_p depends on the bound on F. The estimate of F obtained in Lemma 1 is optimal (smallest and least assumptions) but certainly not practical. Therefore, based on a slight strengthening of the assumptions (Lipschitz is almost differentiable and in applications, this is typically no restriction), we provide better error estimates that take into account the parameter mismatch and the projection.

Assumption 3 The functions $\mathcal{F},\mathcal{G},\mathcal{H}:\Omega\to\mathbb{R}^n$ are differentiable, and there exist some positive constants $M_{\mathcal{F}},M_{\mathcal{G}}$ and $M_{\mathcal{H}}$ such that

$$
\|\mathcal{F}'(z)\|_p\le M_{\mathcal{F}},\ \|\mathcal{G}'(z)\|_p\le M_{\mathcal{G}}\text{ and }\|\mathcal{H}'(z)\|_p\le M_{\mathcal{H}}
$$

for all $z\in\Omega$ and $p=1,2,\infty$.

Lemma 2 *Under the additional Assumption 3, the constant c_p as in Theorem 4 can be replaced by C_p, where*

$$
\begin{aligned}
C_p&=|\alpha|\|(\mathcal{Q}-\hat{\mathcal{Q}})\|_p\beta_p+|1-\alpha|(\|\mathcal{R}\|_p M_{\mathcal{F}}\\
&\quad+\|\mathcal{S}\|_p M_{\mathcal{G}}+\eta_2\|\mathcal{T}\|_p M_{\mathcal{H}})\\
&\quad+\|\mathcal{R}\|_p\|\mathrm{r}_{\mathcal{F}}((\alpha-1)x(t-\varsigma))\|_p\\
&\quad+\|\mathcal{S}\|_p\|\mathrm{r}_{\mathcal{G}}((\alpha-1)x(t-\varsigma))\|_p\\
&\quad+\eta_2\|\mathcal{T}\|_p\|\mathrm{r}_{\mathcal{H}}((\alpha-1)x(t-\varsigma)\|_p\\
&\quad+|\alpha|(\|\hat{\mathcal{R}}-\mathcal{R}\|_p K_{\mathcal{F}}+\|\hat{\mathcal{S}}-\mathcal{S}\|_p K_{\mathcal{G}}+\eta_2\|\hat{\mathcal{T}}-\mathcal{T}\|_p K_{\mathcal{H}}),
\end{aligned}
$$

where $\mathrm{r}_f((\alpha-1)x(t-\varsigma))$ denotes the remainder term of the linear approximation of f that, for fixed x, goes to zero faster than $(\alpha-1)$ approaches zero.

Proof For any $x\in\Omega$, we have

$$
\begin{aligned}
\|F(x,\vartheta_1(t),\vartheta_2(t),\alpha,\varsigma)\|_p&\le\|\alpha(\mathcal{Q}-\hat{\mathcal{Q}})x(t-\varsigma)\|_p\\
&\quad+\|\mathcal{R}\mathcal{F}(\alpha x(t-\varsigma))-\alpha\hat{\mathcal{R}}\mathcal{F}(x(t-\varsigma))\|_p\\
&\quad+\|\mathcal{S}\mathcal{G}(\alpha x(t-\varsigma-\vartheta_1(t)))-\alpha\hat{\mathcal{S}}\mathcal{G}(x(t-\varsigma-\vartheta_1(t)))\|_p\\
&\quad+\Big\|\int_{t-\vartheta_2(t)}^{t}(\mathcal{T}\mathcal{H}(\alpha x(s-\varsigma))-\alpha\hat{\mathcal{T}}\mathcal{H}(x(s-\varsigma)))\Delta s\Big\|.
\end{aligned}
\tag{14}
$$

Now, from Assumption 3, $\mathcal{F}$ is differentiable, and hence, we can write

$$
\begin{aligned}
\mathcal{F}(\alpha x(t-\varsigma))&=\mathcal{F}(x(t-\varsigma)+(\alpha-1)x(t-\varsigma))\\
&=\mathcal{F}(x(t-\varsigma))+(\alpha-1)x(t-\varsigma)\\
&\quad+\mathcal{F}'(x(t-\varsigma)))+\mathrm{r}_{\mathcal{F}}((\alpha-1)x(t-\varsigma)).
\end{aligned}
$$

Therefore, we can calculate

$$
\begin{aligned}
&\mathcal{R}\mathcal{F}(\alpha x(t-\varsigma)\\
&=\mathcal{R}(\mathcal{F}(x(t-\varsigma))+(\alpha-1)x(t-\varsigma)\mathcal{F}'(x(t-\varsigma)))\\
&\quad+\mathrm{r}_{\mathcal{F}}((\alpha-1)x(t-\varsigma))-\alpha\mathcal{R}\mathcal{F}(x(t-\varsigma))\\
&\quad-\alpha(\hat{\mathcal{R}}-\mathcal{R})\mathcal{F}(x(t-\varsigma)).
\end{aligned}
$$

Thus, by using Assumptions 1, 2 and 3

$$
\begin{aligned}
&\|\mathcal{R}\mathcal{F}(\alpha x(t-\varsigma)-\alpha(\mathcal{R}+(\hat{\mathcal{R}}-\mathcal{R}))\mathcal{F}(x(t-\varsigma))\|_p\\
&\le|(1-\alpha)|\|\mathcal{R}\|_p\|(\mathcal{F}'(x(t-\varsigma))x(t-\varsigma))\|_p\\
&\quad+\|\mathcal{R}\|_p\|\mathrm{r}_{\mathcal{F}}((\alpha-1)x(t-\varsigma))\|_p\\
&\quad+|\alpha|\|(\hat{\mathcal{R}}-\mathcal{R})\|_p\|\mathcal{F}(x(t-\varsigma))\|_p\\
&\le|(1-\alpha)|\|\mathcal{R}\|_p M_{\mathcal{F}}+\|\mathcal{R}\|_p\|(\mathrm{r}_{\mathcal{F}}((\alpha-1)x(t-\varsigma))\|_p\\
&\quad+|\alpha|\|(\hat{\mathcal{R}}-\mathcal{R})\|_p K_{\mathcal{F}}.
\end{aligned}
\tag{15}
$$

Similarly, we obtain

$$\begin{aligned}&\|\mathcal{S}\mathcal{G}(\alpha x(t-\varsigma-\vartheta_1(t)))-\alpha\hat{\mathcal{S}}\mathcal{G}(x(t-\varsigma-\vartheta_1(t)))\|_p\\&\le|(1-\alpha)|\|\mathcal{S}\|_pM_{\mathcal{G}}+\|\mathcal{S}\|_p\|\mathrm{r}_{\mathcal{G}}((\alpha-1)x(t-\varsigma))\|_p\\&\quad+|\alpha|\|(\hat{\mathcal{S}}-\mathcal{S})\|_pK_{\mathcal{G}}\end{aligned}\tag{16}$$

and

$$\begin{aligned}&\int_{t-\vartheta_2(t)}^{t}(\|\mathcal{T}\mathcal{H}(\alpha x(s-\varsigma))-\alpha\hat{\mathcal{T}}\mathcal{H}(x(t-\varsigma))\|_p)\Delta s\\&\le\eta_2|(1-\alpha)|\|\mathcal{T}\|_pM_{\mathcal{H}}+\eta_2\|\mathcal{T}\|_p\|\mathrm{r}_{\mathcal{H}}((\alpha-1)x(t-\varsigma))\|_p\\&\quad+\eta_2|\alpha|\|(\hat{\mathcal{T}}-\mathcal{T})\|_pK_{\mathcal{H}}.\end{aligned}\tag{17}$$

Therefore, from the inequalities (14), (15), (16) and (17), we get

$$\|F(x,\vartheta_1(t),\vartheta_2(t),\alpha,\varsigma)\|_p\le C_p.$$

Hence, the result follows. □

Remark 8 Note that the bounds in Lemma 2 scale with the mismatch $\|\hat{\mathcal{R}}-\mathcal{R}\|_p,\|\hat{\mathcal{S}}-\mathcal{S}\|_p$, and $\|\hat{\mathcal{T}}-\mathcal{T}\|_p$. Therefore, the estimate obtained in Lemma 2 is likely sharper than the estimate obtained in Lemma 1 (see Sect. 5).

Remark 9 Assumption 3 is stronger than Assumption 2 but still satisfied by many nonlinear functions and well-known activation functions in applied neural networks, such as *tanh, Sigmoid* or *Logistic*, and *Gaussian*. However, there are some nonlinear functions, like *modulus function*, which are not differentiable at certain points of the domain. Exploring the behaviour of these functions and developing results for such cases could be an interesting direction for future research.

Remark 10 Based on Theorem 4, we can design a control gain matrix that incorporates considerations for parameter mismatches and synchronization error levels. For convenience, we consider $\mathcal{B}=\mathrm{Id}$.

Step 1: Calculate the parameter mismatches bound or uncertainty bound c_p $(or\ C_p)$ from Lemma 1 (or Lemma 2).

Step 2: Chose an appropriate error level $\epsilon_p>0$, and calculate δ_p from $\epsilon_p=\frac{c_p}{\delta_p}$ (or $\frac{C_p}{\delta_p}$).

Step 3: Compute $\mathcal{D}=-\delta_p-L_{\mathcal{G}}\|\mathcal{S}\|_p-\eta_2L_{\mathcal{H}}\|\mathcal{T}\|_p-L_{\mathcal{F}}\|\mathcal{R}\|_p$.

Step 4: Determine the feedback gain matrix $\mathcal{K}$ such that $M_p(\mathcal{Q}-\mathcal{K},\mathbb{T})\le\mathcal{D}$.

We note that the determination of the constants like C_p contain upper and worst-case bounds to the parameter mismatches like $\mathcal{Q}-\hat{\mathcal{Q}}$ so that they naturally cover unmodelled mismatches that are smaller than assumed. Furthermore, the constants that bound the states of the drive system are inferred from a simulation which would also simply include modelling errors in the drive system. Finally, the matrix-measure continuously depends on perturbations in the coefficients as can be seen from the formulas for the particular realizations for the different norms in Table 1. Overall, we can state that the presented procedure is robust with respect to unknown perturbations in the systems.

Next, we provide a remark for different choices of $\mathcal{B}$ and $\mathcal{K}$ as follows.

Remark 11 In Theorem 4,

- if we choose $\mathcal{B}=\mathrm{Id}$, then the values of $\mathcal{M}_{(1,p)}$, $\mathcal{M}_{(2,p)}$, and ϵ_p will be replaced by $-(M_p((\mathcal{Q}-\mathcal{K}),\mathbb{T})+L_{\mathcal{F}}\|\mathcal{R}\|_p\|)$, $L_{\mathcal{G}}\|\mathcal{S}\|_p+\eta_2L_{\mathcal{H}}\|\mathcal{T}\|_p$, and $\frac{c_p}{\delta_p}$, respectively;
- if $\mathcal{K}$ is a time-varying matrix, i.e. $\mathcal{K}=\mathcal{K}(t)$, then the values of $\mathcal{M}_{(1,p)}$ will be replaced by $-(M_p(\mathcal{B}(\mathcal{Q}-\mathcal{K}(t))\mathcal{B}^{-1},\mathbb{T})+L_{\mathcal{F}}\|\mathcal{B}\|_p\|\mathcal{R}\|_p\|\mathcal{B}^{-1}\|_p)$ for all $t\in[0,\infty)_{\mathbb{T}}$;
- if we choose $\mathcal{B}=\mathrm{Id}$ and $\mathcal{K}=\mathcal{K}(t)$, then the values of $\mathcal{M}_{(1,p)}$, $\mathcal{M}_{(2,p)}$, and ϵ_p will be replaced by $-(M_p((\mathcal{Q}-\mathcal{K}(t)),\mathbb{T})+L_{\mathcal{F}}\|\mathcal{R}\|_p\|)$, $L_{\mathcal{G}}\|\mathcal{S}\|_p+\eta_2L_{\mathcal{H}}\|\mathcal{T}\|_p$, and $\frac{c_p}{\delta_p}$, respectively, for all $t\in[0,\infty)_{\mathbb{T}}$.

The next remark discusses some immediate results from the above-obtained results.

Remark 12 Similarly to Theorem 4, Lemma 2, and Remark 11, one can establish the similar results for

- lag quasi-synchronization of the system (1) and (2), when $\alpha=1$;
- projective quasi-synchronization of the system (1) and (2), when $\varsigma=0$;
- quasi-synchronization of the system (1) and (2), when $\alpha=1$ and $\varsigma=0$.

Remark 13 When there are no distributed time delays (i.e. $\vartheta_2(t)=0$), all the above discussed results can be proven by setting the respective terms to zero in the computation of the constants $\mathcal{M}_{(1,p)},\mathcal{M}_{(2,p)}$ and the estimates on the mismatch.

Remark 14 Theorem 4 covers the problem in all generality; therefore, for specific time scales like continuous time or discrete time, the matrix measures in $\mathcal{M}_{(1,p)}$ are readily computed by the known formulas.

Next, some special cases of the considered problem for different time scales including real, discrete, and non-overlapping time intervals are considered and show how our results generalize and extend the existing results.

\\ **Case 1.** For the **continuous-time domain**, i.e. when $\mathbb{T} = \mathbb{R}$, the drive system (1) reduces to

$$x'(t) = \hat{\mathcal{Q}}x(t) + \hat{\mathcal{R}}\mathcal{F}(x(t)) + \hat{\mathcal{S}}\mathcal{G}(x(t-\vartheta_1(t))) + \hat{\mathcal{T}}\int_{t-\vartheta_2(t)}^{t}\mathcal{H}(x(s))ds \tag{18}$$

and the response system (2) reduces to

$$y'(t) = \mathcal{Q}y(t) + \mathcal{R}\mathcal{F}(y(t)) + \mathcal{S}\mathcal{G}(y(t-\vartheta_1(t))) + \mathcal{T}\int_{t-\vartheta_2(t)}^{t}\mathcal{H}(y(s))ds + u(t), \tag{19}$$

where $t \in [0,\infty)$ and the remaining parameters are equal to those defined previously.

Remark 15 As far as we know, the PLQS of the continuous-time system (18)–(19) using the Halanay inequality and matrix-measure approach has not yet been investigated in the existing literature. Hence, the findings presented in this paper are entirely novel, even in the context of continuous-time systems. A few authors [29, 34] have investigated different synchronization results for the system (18)–(19) by using the different techniques. Notably, our results are particularly significant when $\varsigma = 0$, where they become the main outcomes of [34]. Further, in contrast to the impulsive control approach utilized in [29], we utilize a feedback controller and provide simpler criteria for achieving PLQS. Our numerical simulations show that to achieve the same error bounds, our proposed method greatly reduces the required feedback gain as compared to [29] (see Example 2), underscoring the efficacy of our approach.

Remark 16 The synchronization results for the continuous-time system (18)–(19) without distributed time delay, i.e. when $\vartheta_2(t) = 0$, have been investigated in [28, 32, 33, 35]. In particular, if $\alpha = 1$, our results coincide with those of [35]. Further, in comparison with the intermittent technique developed in [33], our results significantly reduce the required feedback gain to achieve the same error bound, as shown in Example 3. This further demonstrates that the results of this paper are non-trivial extensions and generalizations of the existing results.

Case 2. For the $h-$**difference discrete-time domain**, i.e. when $\mathbb{T} = h\mathbb{Z}$, $h > 0$, the drive system (1) reduces to

$$x(t+h) = x(t) + h(\hat{\mathcal{Q}}x(t) + \hat{\mathcal{R}}\mathcal{F}(x(t)) + \hat{\mathcal{S}}\mathcal{G}(x(t-\vartheta_1(t))) + \hat{\mathcal{T}}\int_{t-\vartheta_2(t)}^{t}\mathcal{H}(x(s))\Delta s) \tag{20}$$

and the response system (2) reduces to

$$y(t+h) = y(t) + h(\mathcal{Q}y(t) + \mathcal{R}\mathcal{F}(y(t)) + \mathcal{S}\mathcal{G}(y(t-\vartheta_1(t))) + \mathcal{T}\int_{t-\vartheta_2(t)}^{t}\mathcal{H}(y(s))\Delta s + u(t)), \tag{21}$$

where $t \in [0,\infty)_{h\mathbb{Z}}$.

Remark 17 The discrete-time systems have been studied in [13, 18, 20], but to the best of our knowledge, there is no paper that discussed the PLQS results for the discrete-type system (20)–(21). However, we have formulated our problem by using the time scales theory; therefore, our results can also be applied to the discrete-time systems of the form (20)–(21), as demonstrated in Case 2 of Example 1.

Case 3. For the **mixed time domain** $\mathbb{T} = hP_{c,d}$, i.e. $\mathbb{T} = \cup_{l=0}^{\infty}h[l(c+d), l(c+d)+d]$, $h, c, d > 0$, which is different from the traditional discrete-time domain and continuous-time domain, the drive system (1) becomes

$$\begin{cases} x'(t) = \widehat{\mathcal{Q}}x(t) + \widehat{\mathcal{R}}\mathcal{F}(x(t)) + \widehat{\mathcal{S}}\mathcal{G}(x(t-\vartheta_1(t))) \\ \qquad + \widehat{\mathcal{T}}\int_{t-\vartheta_2(t)}^{t}\mathcal{H}(x(s))ds,\ t \in h\mathbb{P}_{c,d}\backslash\cup_{l=0}^{\infty}h\{l(c+d)+d\}, \\ x(t+hc) = x(t) + hc(\widehat{\mathcal{Q}}x(t) + \widehat{\mathcal{R}}\mathcal{F}(x(t)) + \widehat{\mathcal{S}}\mathcal{G}(x(t-\vartheta_1(t))) \\ \qquad + \widehat{\mathcal{T}}\int_{t-\vartheta_2(t)}^{t}\mathcal{H}(x(s))\Delta s),\ t = \cup_{l=0}^{\infty}h\{l(c+d)+d\} \end{cases} \tag{22}$$

and the response system (2) becomes

$$\begin{cases} y'(t) = \mathcal{Q}y(t) + \mathcal{R}\mathcal{F}(y(t)) + \mathcal{S}\mathcal{G}(y(t-\vartheta_1(t))) \\ \qquad + \mathcal{T}\int_{t-\vartheta_2(t)}^{t}\mathcal{H}(y(s))ds + u(t),\ t \in h\mathbb{P}_{c,d}\backslash\cup_{l=0}^{\infty}h\{l(c+d)+d\}, \\ y(t+hc) = y(t) + hc(\mathcal{Q}y(t) + \mathcal{R}\mathcal{F}(y(t)) + \mathcal{S}\mathcal{G}(y(t-\vartheta_1(t))) \\ \qquad + \mathcal{T}\int_{t-\vartheta_2(t)}^{t}\mathcal{H}(y(s))\Delta s + u(t)),\ t = \cup_{l=0}^{\infty}h\{l(c+d)+d\}. \end{cases} \tag{23}$$

We are ending up this section by giving the final remark as follows.

Remark 18 Standard and generalized matrix-measure theory can be used to establish results for regular time-domain systems, such as continuous and discrete-time systems. However, for irregular time-domain systems like (22) and (23), these results cannot be directly studied using discrete-time and continuous-time system theories. Instead, the time scales and unified matrix-measure theory can be used to study these results easily (see case 3 of Example 1).

5 Illustrative examples

In this section, we provide three examples to illustrate the obtained results for different time domains. Whereas the first example is tailored to best illustrate the potential of our theoretical results with respect to arbitrary time domains, the second example is borrowed from [29] to show the general applicability of our methods. In the final example, we consider the Lu oscillator from [33] and show that our results can be applied to a variety of dynamical systems.

Example 1 Consider the following coefficients for the drive system (1) and the response system (2)

$$\hat{\mathcal{Q}} = \begin{bmatrix} -0.5 & 0.0 \\ 0.0 & -0.4 \end{bmatrix}, \ \hat{\mathcal{R}} = \begin{bmatrix} 0.4 & 0.4 \\ 0.4 & 0.3 \end{bmatrix},$$
$$\hat{\mathcal{S}} = \begin{bmatrix} -0.4 & 0.1 \\ -0.2 & 0.5 \end{bmatrix}, \ \hat{\mathcal{T}} = \begin{bmatrix} 0.2 & -0.1 \\ 0.1 & -0.4 \end{bmatrix},$$
$$\mathcal{Q} = \begin{bmatrix} -0.51 & 0.0 \\ 0.0 & -0.41 \end{bmatrix}, \ \mathcal{R} = \begin{bmatrix} 0.401 & 0.401 \\ 0.401 & 0.311 \end{bmatrix},$$
$$\mathcal{S} = \begin{bmatrix} -0.401 & 0.11 \\ -0.21 & 0.5001 \end{bmatrix}, \ \mathcal{T} = \begin{bmatrix} 0.201 & -0.101 \\ 0.101 & -0.4001 \end{bmatrix},$$
$$\mathcal{F}(x(\cdot)) = \mathcal{G}(x(\cdot)) = \begin{bmatrix} 0.7\tanh(x_1(\cdot)) \\ 0.8\tanh(x_2(\cdot)) \end{bmatrix},$$
$$\mathcal{H}(x(\cdot)) = \begin{bmatrix} 0.8\tanh(x_1(\cdot)) \\ 0.7\tanh(x_2(\cdot)) \end{bmatrix},$$
$$\hat{\phi}(s) = \begin{bmatrix} -0.2 \\ -0.1 \end{bmatrix}, \ \phi(s) = \begin{bmatrix} 0.1 \\ 0.2 \end{bmatrix} \text{ for } s \in [-\eta, 0]_{\mathbb{T}},$$
$$\alpha = 0.5, \ \mathcal{B} = \begin{bmatrix} 1 & 0 \\ 0 & 1 \end{bmatrix}.$$

Clearly, for the considered coefficients, Assumption 1 holds. Also, one can see that $\mathcal{F}, \mathcal{G}$, and $\mathcal{H}$ satisfy Assumption 2 and Assumption 3. Now, we consider the following three different time domains as follows.

Case 1. $\mathbb{T} = \mathbb{R}$, i.e. $\mu(t) = 0$ for all t. We set $\vartheta_1(t) = \vartheta_2(t) = \frac{\exp(t)}{2+\exp(t)}$ and $\varsigma = 0.4$; then, $\eta = 1$. The synchronization errors and error norm between the drive system (1) and the response system (2) without feedback controller are shown in Fig. 3.

Now, for the coupling matrix

$$\mathcal{K} = \begin{bmatrix} 3.81 & 0.0 \\ 0.0 & 3.91 \end{bmatrix},$$

we can calculate

$$\mathcal{M}_{(2,1)} = 0.8897, \ \mathcal{M}_{(2,2)} = 0.8505, \ \mathcal{M}_{(2,\infty)} = 0.9690$$

and

$$\Upsilon_1(\mathcal{Q} - \mathcal{K}) = -4.32, \ \Upsilon_2(\mathcal{Q} - \mathcal{K}) = -8.64, \ \Upsilon_\infty(\mathcal{Q} - \mathcal{K}) = -4.32.$$

Hence,

$$\mathcal{M}_{(1,1)} = 3.6784, \quad \mathcal{M}_{(1,2)} = 8.0327, \text{ and } \mathcal{M}_{(1,\infty)} = 3.6784.$$

Therefore, we can see that $-\mathcal{M}_{(1,p)} \in \mathcal{R}^+$ for $p \in \{1, 2, \infty\}$ and

$$\mathcal{M}_{(1,1)} - \mathcal{M}_{(2,1)} \geq 2.7887 > 0,$$
$$\mathcal{M}_{(1,2)} - \mathcal{M}_{(2,2)} \geq 7.1822 > 0,$$
$$\mathcal{M}_{(1,\infty)} - \mathcal{M}_{(2,\infty)} \geq 2.70940.$$

Also, for $k = 0.5$ and $p \in \{1, 2, \infty\}$, the inequality $k\mathcal{M}_{(1,p)} - \mathcal{M}_{(2,p)} > 0$ holds. Thus, all of the requirements of Theorem 4 and Lemma 2 are satisfied, and as a result, the drive system (1) and the response system (2) are projective lag quasi-synchronized. The synchronization errors and error norm between the drive system (1) and the response system (2) with feedback controller (3) are shown in Fig. 4.

The theoretical error bounds for different values of p are given in Table 2. Clearly, the theoretical error bound obtained from Lemma 2 is fairly close to the computed error as shown in Fig. 4.

Case 2. $\mathbb{T} = 0.2\mathbb{Z}$, i.e. $\mu(t) = 0.2$ for all $t \in 0.2\mathbb{Z}$. We set $\vartheta_1(t) = \vartheta_2(t) = 0.2$ and $\varsigma = 0.4$; then, $\eta = 0.2$. The synchronization errors and error norm between the drive system (1) and the response system (2) without feedback controller (3) are shown in Fig. 5.

Now, for the coupling matrix

$$\mathcal{K} = \begin{bmatrix} 4.49 & 0.0 \\ 0.0 & 4.59 \end{bmatrix},$$

we can calculate

$$\mathcal{M}_{(2,1)} = 0.5690, \ \mathcal{M}_{(2,2)} = 0.5674, \ \mathcal{M}_{(2,\infty)} = 0.6483$$

and

$$\omega_1(\mathcal{Q} - \mathcal{K}) = -5.0, \ \omega_2(\mathcal{Q} - \mathcal{K}) = -5.0, \ \omega_\infty(\mathcal{Q} - \mathcal{K}) = -5.0.$$

Hence,

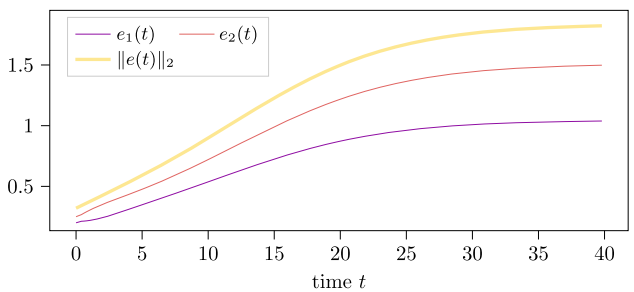

Fig. 3 Trajectories of the errors e_1, e_2, and error norm $\|e\|_2$ of the uncontrolled system when $\mathbb{T} = \mathbb{R}$

$$\mathcal{M}_{(1,1)} = 4.3584, \quad \mathcal{M}_{(1,2)} = 4.3927, \text{ and } \mathcal{M}_{(1,\infty)} = 4.3584.$$

Therefore, we can see that $-\mathcal{M}_{(1,p)} \in \mathcal{R}^+$ for $p \in \{1, 2, \infty\}$ and

$$\mathcal{M}_{(1,1)} - \mathcal{M}_{(2,1)} \geq 3.7894 > 0,$$
$$\mathcal{M}_{(1,2)} - \mathcal{M}_{(2,2)} \geq 3.8253 > 0,$$
$$\mathcal{M}_{(1,\infty)} - \mathcal{M}_{(2,\infty)} \geq 3.7101 > 0.$$

Also, for $k = 0.5$ and $p \in \{1, 2, \infty\}$, the inequality $k\mathcal{M}_{(1,p)} - \mathcal{M}_{(2,p)} > 0$ holds. Thus, all of the requirements of Theorem 4 and Lemma 2 are satisfied, and as a result, the drive system (1) and the response system (2) are projective lag quasi-synchronized. The synchronization errors and error norm between the drive system (1) and the response system (2) with feedback controller (3) are shown in Fig. 6.

The theoretical error bounds for different values of p are given in Table 3. Here also, the theoretical error bound obtained from Lemma 2 is fairly close to the computed error as shown in Fig. 6.

Case 3. $\mathbb{T} = \mathcal{P} = [-1, 0] \cup_{l=0}^{\infty} 0.5[l, (l + 0.7)]$. Here, $\mu(t)$ is given by

$$\mu(t) = \begin{cases} 0, & t \in [-1, 0] \cup_{l=0}^{\infty} [0.5l, 0.5(l + 0.7)), \\ 0.15, & t = \cup_{l=0}^{\infty} \{0.5(l + 0.7)\}. \end{cases}$$

We set $\vartheta_1(t) = \vartheta_2(t) = 0.5$ and $\varsigma = 1$; then, $\eta = 0.5$. The synchronization errors and error norm between the drive system (1) and the response system (2) without feedback controller (3) are shown in Fig. 7.

Now, for the coupling matrix

$$\mathcal{K} = \begin{bmatrix} 6.15 & 0.0 \\ 0.0 & 6.25 \end{bmatrix},$$

we can calculate

$$\mathcal{M}_{(2,1)} = 0.6892, \ \mathcal{M}_{(2,2)} = 0.6736, \ \mathcal{M}_{(2,\infty)} = 0.7685$$

and

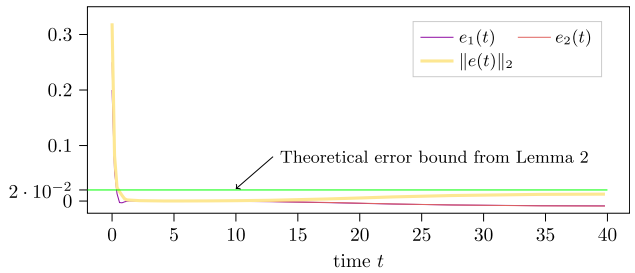

Fig. 4 Trajectories of the errors e_1, e_2, and error norm $\|e\|_2$ of the controlled system when $\mathbb{T} = \mathbb{R}$

Table 2 Error bounds from Theorem 4 and Lemma 2 when $\mathbb{T} = \mathbb{R}$

p	c_p	C_p	δ_p	$\epsilon_p = \frac{c_p}{\delta_p}$	$\epsilon_p = \frac{C_p}{\delta_p}$
1	2.2998	0.1469	2.7887	0.8247	0.0526
2	2.1861	0.1374	7.1822	0.3044	0.02
∞	2.4156	0.1490	2.7094	0.8916	0.054

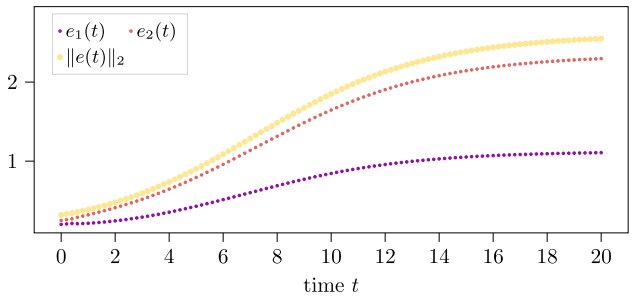

Fig. 5 Trajectories of the errors e_1, e_2, and error norm $\|e\|_2$ of the uncontrolled system when $\mathbb{T} = \frac{1}{5}\mathbb{Z}$

$$M_1((\mathcal{Q} - \mathcal{K}), \mathcal{P}) = -6.66, \ M_2((\mathcal{Q} - \mathcal{K}), \mathcal{P}) = -6.66,$$
$$M_\infty((\mathcal{Q} - \mathcal{K}), \mathcal{P}) = -6.66.$$

Hence,

$$\mathcal{M}_{(1,1)} = 6.0184, \quad \mathcal{M}_{(1,2)} = 6.0527, \text{ and}$$
$$\mathcal{M}_{(1,\infty)} = 6.0184.$$

Therefore, we can see that $-\mathcal{M}_{(1,p)} \in \mathcal{R}^+$ for $p \in \{1, 2, \infty\}$ and

$$\mathcal{M}_{(1,1)} - \mathcal{M}_{(2,1)} \geq 5.3292 > 0,$$
$$\mathcal{M}_{(1,2)} - \mathcal{M}_{(2,2)} \geq 5.3791 > 0,$$
$$\mathcal{M}_{(1,\infty)} - \mathcal{M}_{(2,\infty)} \geq 5.2499 > 0.$$

Also, for $k = 0.5$ and $p \in \{1, 2, \infty\}$, the inequality $k\mathcal{M}_{(1,p)} - \mathcal{M}_{(2,p)} > 0$ holds. Thus, all of the requirements of Theorem 4 and Lemma 2 are satisfied, and as a result, the drive system (1) and the response system (2) are projective lag quasi-synchronized. The synchronization errors

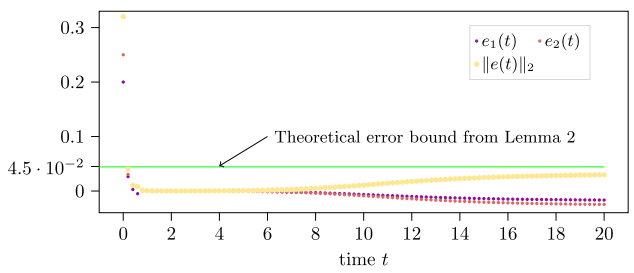

Fig. 6 Trajectories of the errors e_1, e_2, and error norm $\|e\|_2$ of the controlled system when $\mathbb{T} = \frac{1}{5}\mathbb{Z}$

Table 3 Error bounds from Theorem 4 and Lemma 2 when $\mathbb{T} = \frac{1}{5}\mathbb{Z}$

p	c_p	C_p	δ_p	$\epsilon_p = \frac{c_p}{\delta_p}$	$\epsilon_p = \frac{C_p}{\delta_p}$
1	1.8223	0.1770	3.7894	0.4809	0.0467
2	1.7673	0.1696	3.8253	0.4620	0.0443
∞	1.9416	0.1849	3.7101	0.5233	0.04983

and error norm between the drive system (1) and the response system (2) with feedback controller (3) are shown in Fig. 8.

The theoretical error bounds for different values of p are given in Table 4. In this case also, the theoretical error bound obtained from Lemma 2 is fairly close to the computed error as shown in Fig. 8.

Example 2 Consider the continuous-time case of the drive and response systems (18)–(19) with the following coefficients as in [29]

$$\hat{\mathcal{Q}} = \begin{bmatrix} -1.0 & 0.0 \\ 0.0 & -1.0 \end{bmatrix}, \hat{\mathcal{R}} = \begin{bmatrix} 2.0 & -0.1 \\ 5.0 & 4.5 \end{bmatrix},$$
$$\hat{\mathcal{S}} = \begin{bmatrix} -1.5 & -0.1 \\ -0.2 & -4.0 \end{bmatrix}, \hat{\mathcal{T}} = \begin{bmatrix} -0.3 & 0.1 \\ 0.1 & -0.2 \end{bmatrix},$$
$$\mathcal{Q} = \begin{bmatrix} -1.0 & 0.0 \\ 0.0 & -1.0 \end{bmatrix}, \mathcal{R} = \begin{bmatrix} 1.8 & -0.15 \\ -0.52 & 3.5 \end{bmatrix},$$
$$\mathcal{S} = \begin{bmatrix} -1.7 & -0.12 \\ -0.26 & -2.5 \end{bmatrix}, \mathcal{T} = \begin{bmatrix} 0.6 & 0.15 \\ 2.0 & -0.12 \end{bmatrix},$$
$$\mathcal{F}(x(\cdot)) = \mathcal{G}(x(\cdot)) = \mathcal{H}(x(\cdot)) = \begin{bmatrix} \tanh(x_1(\cdot)) \\ \tanh(x_2(\cdot)) \end{bmatrix}, \mathcal{B} = \begin{bmatrix} 1 & 0 \\ 0 & 1 \end{bmatrix},$$
$$\vartheta_1(t) = 1, \vartheta_2(t) = 0.2, \alpha = 0.5, \hat{\phi}(s) = \begin{bmatrix} 0.01 \\ 0.1 \end{bmatrix},$$
$$\phi(s) = \begin{bmatrix} 0.02 \\ 0.01 \end{bmatrix} \text{ for } s \in [-1, 0].$$

Clearly, for the considered coefficients, Assumption 1 holds. Also, one can see that $\mathcal{F}, \mathcal{G}$, and $\mathcal{H}$ satisfy Assumption 2 and Assumption 3. The synchronization errors and error norm between the drive system (1) and the response system (2) without feedback controller are shown in Fig. 9.

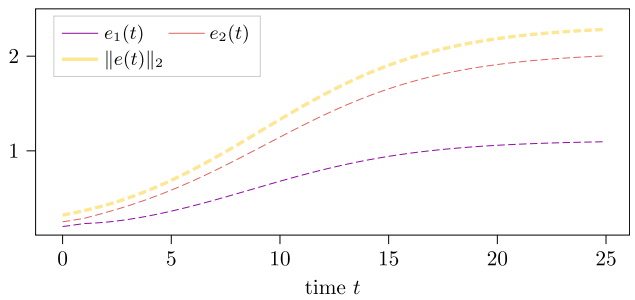

Fig. 7 Trajectories of the errors e_1, e_2, and error norm $\|e\|_2$ of the uncontrolled system when $\mathbb{T} = \mathcal{P}$

Now, for the coupling matrix

$$\mathcal{K} = \begin{bmatrix} 10.1557 & 0.0 \\ 0.0 & 10.1557 \end{bmatrix},$$

we can calculate $\mathcal{M}_{(2,2)} = 2.9619$ and $\Upsilon_2(\mathcal{Q} - \mathcal{K}) = -22.3114$. Hence, $\mathcal{M}_{(1,2)} = 15.8442$. Therefore, we can see that $\mathcal{M}_{(1,2)} - \mathcal{M}_{(2,2)} = 12.8824 > 0$ and $-\mathcal{M}_{(1,2)} \in \mathcal{R}^+$. Also, for $k = 0.5$, the inequality $k\mathcal{M}_{(1,2)} - \mathcal{M}_{(2,2)} > 0$ holds. Thus, all of the requirements of Theorem 4 and Lemma 2 are satisfied, and as a result, the drive system (1) and the response system (2) are projective lag quasi-synchronized. The synchronization errors and error norm between the drive system (1) and the response system (2) with feedback controller (3) are shown in Fig. 10.

Further, for $p = 2$, we can calculate $C_2 = 3.1471$. Hence, the theoretical error bound $\epsilon_2 = \frac{C_2}{\delta_2}$ is 0.2443. Comparing the results quantitatively, we note that to achieve the error bound 0.2443, we used the feedback gain $\mathcal{K} = \text{diag}\{10.1557, 10.1557\}$, while to achieve the same error bound, the authors in [29] used a gain of $\mathcal{K} = \text{diag}\{20, 20\}$, which is approximate double of our gain.

Finally, we present our third example as follows.

Example 3 Consider the continuous-time Lu oscillator given by the drive and response systems (18)–(19) with the following coefficients as in [33]

$$\hat{\mathcal{Q}} = \begin{bmatrix} -1.0 & 0.0 \\ 0.0 & -1.0 \end{bmatrix}, \hat{\mathcal{R}} = \begin{bmatrix} 2.0 & -0.1 \\ 5.0 & 3.2 \end{bmatrix},$$
$$\hat{\mathcal{S}} = \begin{bmatrix} -1.5 & -0.1 \\ -0.18 & -2.5 \end{bmatrix},$$
$$\mathcal{Q} = \begin{bmatrix} -0.99 & 0.0 \\ 0.0 & -1.1 \end{bmatrix}, \mathcal{R} = \begin{bmatrix} 2.1 & -0.1 \\ -0.51 & 3.1 \end{bmatrix},$$
$$\mathcal{S} = \begin{bmatrix} -1.5 & -0.11 \\ -0.16 & -2.4 \end{bmatrix},$$
$$\mathcal{F}(x(\cdot)) = \mathcal{G}(x(\cdot)) = \begin{bmatrix} \tanh(x_1(\cdot)) \\ \tanh(x_2(\cdot)) \end{bmatrix}, \mathcal{B} = \begin{bmatrix} 1 & 0 \\ 0 & 1 \end{bmatrix},$$
$$\vartheta_1(t) = 1, \vartheta_2(t) = 0.0, \alpha = 0.9, \varsigma = 0.02, p = 2,$$
$$\hat{\phi}(s) = \begin{bmatrix} 0.2 \\ -0.3 \end{bmatrix}, \phi(s) = \begin{bmatrix} -0.1 \\ 0.1 \end{bmatrix} \text{ for } s \in [-1, 0].$$

Clearly, for the considered coefficients, Assumption 1 holds. Also, one can see that $\mathcal{F}, \mathcal{G}$, and $\mathcal{H}$ satisfy Assumption 2 and Assumption 3. The synchronization errors and error norm between the drive system (1) and the response system (2) without feedback controller are shown in Fig. 11.

Now, for the coupling matrix

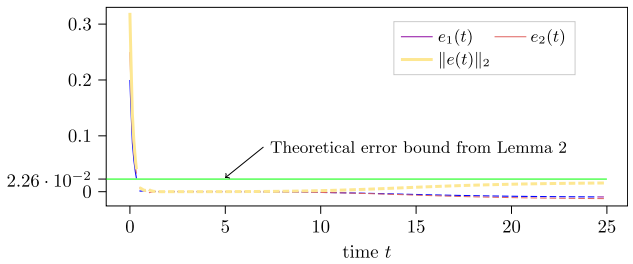

Fig. 8 Trajectories of the errors e_1, e_2, and error norm $\|e\|_2$ of the controlled system when $\mathbb{T} = \mathcal{P}$

Table 4 Error bounds from Theorem 4 and Lemma 2 when $\mathbb{T} = \mathcal{P}$

p	c_p	C_p	δ_p	$\epsilon_p = \frac{c_p}{\delta_p}$	$\epsilon_p = \frac{C_p}{\delta_p}$
1	1.9994	0.1290	5.3292	0.3752	0.0242
2	1.9233	0.1216	5.3791	0.3575	0.0226
∞	2.1187	0.1311	5.2499	0.4036	0.0249

$$\mathcal{K} = \begin{bmatrix} 10.4848 & 0.0 \\ 0.0 & 10.3748 \end{bmatrix},$$

we can calculate $\mathcal{M}_{(2,2)} = 2.42$ and $\Upsilon_2(\mathcal{Q} - \mathcal{K}) = -22.9496$. Hence, $\mathcal{M}_{(1,2)} = 16.6950$. Therefore, we can see that $\mathcal{M}_{(1,2)} - \mathcal{M}_{(2,2)} = 14.2750 > 0$ and $-\mathcal{M}_{(1,2)} \in \mathcal{R}^+$. Also, for $k = 0.5$, the inequality $k\mathcal{M}_{(1,2)} - \mathcal{M}_{(2,2)} > 0$ holds. Thus, all of the requirements of Theorem 4 and Lemma 2 are satisfied, and as a result, the drive system (1) and the response system (2) are projective lag quasi-synchronized. The synchronization errors and error norm between the drive system (1) and the response system (2) with feedback controller (3) are shown in Fig. 12.

Further, for $p = 2$, we can calculate $C_2 = 3.5259$. Hence, the theoretical error bound $\epsilon_2 = \frac{C_2}{\delta_2}$ is 0.2470. Comparing the results quantitatively, we note that to achieve the error bound 0.2470, we used the feedback gain $\mathcal{K} = \text{diag}\{10.4848, 10.3848\}$, while to achieve the same

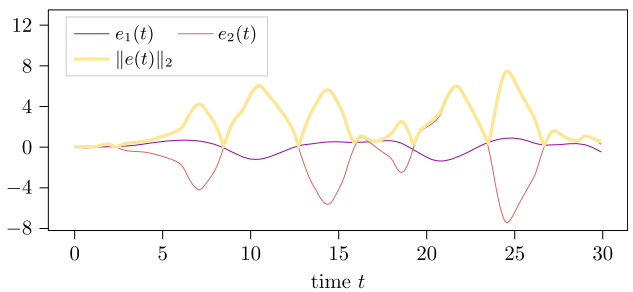

Fig. 9 Trajectories of the errors e_1, e_2, and error norm $\|e\|_2$ of the uncontrolled system

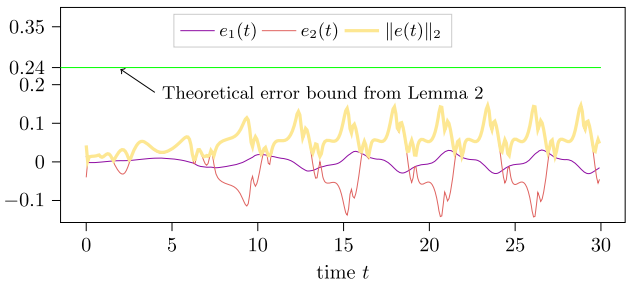

Fig. 10 Trajectories of the errors e_1, e_2, and error norm $\|e\|_2$ of the controlled system

error bound, the authors in [33] used the intermittent control technique with a feedback gain of $\mathcal{K} = \text{diag}\{40, 40\}$, which is approximate four times of our gain.

Remark 19 Previous works, such as [28, 29, 32–35], have considered similar types of examples on either continuous or discrete-time domains. To the best of our knowledge, there is currently no other example in the literature that has addressed PLQS of coupled systems on hybrid-type time domains (as presented in case 3 of Example 1).

Remark 20 In this paper, we have derived protocols for achieving asymptotic quasi-synchronization. However, it is important to note that these protocols only guarantee convergence with an infinite settling time. In order to address this limitation, an interesting future direction could be to investigate the finite-time quasi-synchronization, where the synchronization is achieved within a specific finite-time period instead of an infinite duration. Furthermore, the continuous feedback controller we used in our approach can be costly in terms of implementation and computational resources. Therefore, another potential future direction could be to develop alternative controllers, like impulsive controllers and event-triggered controllers which have the advantage of reducing implementation and computational costs compared to continuous feedback control.

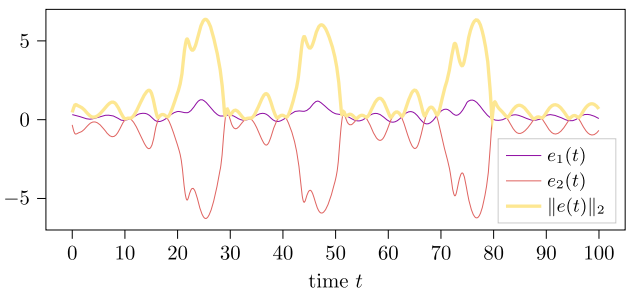

Fig. 11 Trajectories of the errors e_1, e_2, and error norm $\|e\|_2$ of the uncontrolled system

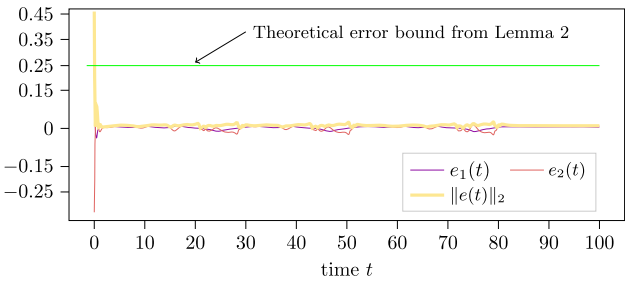

Fig. 12 Trajectories of the errors e_1, e_2, and error norm $\|e\|_2$ of the controlled system

6 Conclusions

In this study, we have presented a feedback control law that successfully establishes projective lag quasi-synchronization for coupled dynamical systems with parameter mismatches and mixed time-varying delays on arbitrary time domains. More precisely, we first formulated the problem on time scales, allowing the results to be valid for arbitrary time domains. Next, we derived various sufficient conditions for projective lag quasi-synchronization and obtained corresponding error bounds. Additionally, by setting some particular values to the parameters, we provided different conditions for projective quasi-synchronization, quasi-synchronization, and lag synchronization. Our study has also extended and refined existing results by generalizing them using the time scales theory. The analytical outcomes have been validated using time scales calculus, unified matrix-measure, and generalized Halanay inequality. In the last, we provided some numerical examples for different time domains and showed that the error bounds obtained analytically are very close to the simulated error bounds.

Overall, this study provides a comprehensive understanding of the problem of projective lag quasi-synchronization and offers a generic solution for synchronizing parameter mismatched coupled dynamical systems with mixed time-varying delays on continuous, discrete and also arbitrary time domains. It can be used as a foundation for future research in the field of synchronization of deterministic and stochastic dynamical systems. An immediate valuable extension would be the inclusion of impulsive effects with time-dependent delays. Furthermore, a promising application where memory terms, delays, and on-off behaviour as it can be naturally modelled by time scales are relevant lies in the synchronization of connected memristors [16].

Acknowledgements The authors are grateful to anonymous reviewers whose valuable comments helped improve the quality of this study.

Author contributions All authors contributed equally and significantly in writing this article. All authors read and approved the final manuscript.

Funding Open Access funding enabled and organized by Projekt DEAL. The work by Jan Heiland and Peter Benner was supported by the German Research Foundation (DFG) Research Training Group 2297 “Mathematical Complexity Reduction (MathCoRe)”.

Data availability No data available.

Declarations

Conflict of interest The authors declare that they have no conflict of interest.

References

1. Pecora LM, Carroll TL (1990) Synchronization in chaotic systems. Phys Rev Lett 64(8):821
2. Chen J, Jiao L, Wu J, Wang X (2010) Projective synchronization with different scale factors in a driven-response complex network and its application in image encryption. Nonlinear Anal Real World Appl 11(4):3045–3058
3. Xie Q, Chen G, Bollt EM (2002) Hybrid chaos synchronization and its application in information processing. Math Comput Model 35(1–2):145–163
4. Lu J, Wu X, Lü J (2002) Synchronization of a unified chaotic system and the application in secure communication. Phys Lett A 305(6):365–370
5. Li T, Sm Fei, Kj Zhang (2008) Synchronization control of recurrent neural networks with distributed delays. Phys A 387(4):982–996
6. Li T, Sm Fei, Zhu Q, Cong S (2008) Exponential synchronization of chaotic neural networks with mixed delays. Neurocomputing 71(13–15):3005–3019
7. Aliabadi F, Majidi MH, Khorashadizadeh S (2022) Chaos synchronization using adaptive quantum neural networks and its application in secure communication and cryptography. Neural Comput Appl 34(8):6521–6533
8. Du H, Zeng Q, Wang C, Ling M (2010) Function projective synchronization in coupled chaotic systems. Nonlinear Anal Real World Appl 11(2):705–712
9. Sun M, Lyu D, Jia Q (2022) Event-triggered leader-following synchronization of delayed dynamical networks with intermittent coupling. Neural Comput Appl 34:6163–6170
10. Yang X, Li X, Duan P (2022) Finite-time lag synchronization for uncertain complex networks involving impulsive disturbances. Neural Comput Appl 34(7):5097–5106
11. He W, Cao J (2009) Exponential synchronization of chaotic neural networks: a matrix measure approach. Nonlinear Dyn 55(1):55–65
12. Cao J, Wan Y (2014) Matrix measure strategies for stability and synchronization of inertial BAM neural network with time delays. Neural Netw 53:165–172

13. Xiao Q, Huang T, Zeng Z (2018) Global exponential stability and synchronization for discrete-time inertial neural networks with time delays: a timescale approach. IEEE Trans Neural Netw Learn Syst 30(6):1854–1866
14. Li N, Cao J (2015) Lag synchronization of memristor-based coupled neural networks via ω-measure. IEEE Trans Neural Netw Learn Syst 27(3):686–697
15. Chen X, Lin D, Lan W (2020) Global dissipativity of delayed discrete-time inertial neural networks. Neurocomputing 390:131–138
16. Gambuzza LV, Buscarino A, Fortuna L, Frasca M (2015) Memristor-based adaptive coupling for consensus and synchronization. IEEE Trans Circuits Syst I Regul Pap 62(4):1175–1184
17. Wu ZG, Shi P, Su H, Chu J (2012) Exponential synchronization of neural networks with discrete and distributed delays under time-varying sampling. IEEE Trans Neural Netw Learn Syst 23(9):1368–1376
18. Ouannas A (2015) A new generalized-type of synchronization for discrete-time chaotic dynamical systems. J Comput Nonlinear Dyn 10(6):061019
19. He W, Qian F, Lam J, Chen G, Han QL, Kurths J (2015) Quasi-synchronization of heterogeneous dynamic networks via distributed impulsive control: error estimation, optimization and design. Automatica 62:249–262
20. Ding S, Wang Z, Rong N (2020) Intermittent control for quasisynchronization of delayed discrete-time neural networks. IEEE Trans Cybern 51(2):862–873
21. Shahverdiev E, Sivaprakasam S, Shore K (2002) Lag synchronization in time-delayed systems. Phys Lett A 292(6):320–324
22. Mainieri R, Rehacek J (1999) Projective synchronization in three-dimensional chaotic systems. Phys Rev Lett 82(15):3042
23. Hoang TM, Nakagawa M (2008) A secure communication system using projective-lag and/or projective-anticipating synchronizations of coupled multidelay feedback systems. Chaos Solitons Fractals 38(5):1423–1438
24. Li GH (2009) Projective lag synchronization in chaotic systems. Chaos Solitons Fractals 41(5):2630–2634
25. Chai Y, Chen LQ (2012) Projective lag synchronization of spatiotemporal chaos via active sliding mode control. Commun Nonlinear Sci Numer Simul 17(8):3390–3398
26. Zheng M, Wang Z, Li L, Peng H, Xiao J, Yang Y et al (2018) Finite-time generalized projective lag synchronization criteria for neutral-type neural networks with delay. Chaos Solitons Fractals 107:195–203
27. Chai XL, Gan ZH (2019) Function projective lag synchronization of chaotic systems with certain parameters via adaptive-impulsive control. Int J Autom Comput 16(2):238–247
28. Han Q, Li C, Huang J (2010) Estimation on error bound of lag synchronization of chaotic systems with time delay and parameter mismatch. J Vib Control 16(11):1701–1711
29. Kumar R, Sarkar S, Das S, Cao J (2019) Projective synchronization of delayed neural networks with mismatched parameters and impulsive effects. IEEE Trans on Neural Netw Learn Syst 31(4):1211–1221
30. Kumar R, Das S (2020) Weak, modified and function projective synchronization of Cohen-Grossberg neural networks with mixed time-varying delays and parameter mismatch via matrix measure approach. Neural Comput Appl 32:7321–7332
31. Zou W, Wen X, Guo J, Xiang Z (2023) Novel reference trajectory-based finite-time consensus protocols for multiagent systems with non-identical nonlinear dynamics. IEEE Trans Netw Sci Eng 10(2):1107–1118
32. Huang J, Li C, Huang T, Han Q (2013) Lag quasisynchronization of coupled delayed systems with parameter mismatch by periodically intermittent control. Nonlinear Dyn 71(3):469–478
33. Yuan X, Li C, Huang T (2017) Projective lag synchronization of delayed chaotic systems with parameter mismatch via intermittent control. Int J Nonlinear Sci 23(1):3–10
34. Chen S, Cao J (2012) Projective synchronization of neural networks with mixed time-varying delays and parameter mismatch. Nonlinear Dyn 67(2):1397–1406
35. He W, Qian F, Han QL, Cao J (2011) Lag quasi-synchronization of coupled delayed systems with parameter mismatch. IEEE Trans Circuits Syst I Regul Pap 58(6):1345–1357
36. Huang J, Li C, Zhang W, Wei P (2014) Weak projective lag synchronization of neural networks with parameter mismatch. Neural Comput Appl 24(1):155–160
37. Feng CF, Yang HJ (2020) Projective-lag synchronization scheme between two different discrete-time chaotic systems. Int J Non-Linear Mech 121:103451
38. Xiao Q, Huang T (2019) Quasisynchronization of discrete-time inertial neural networks with parameter mismatches and delays. IEEE Trans Cybern 51(4):2290–2295
39. Bohner M, Peterson A (2001) Dynamic equations on time scales. Birkhäuser, Boston
40. Hilger S (1988) Ein Maßkettenkalkül mit Anwendung auf Zentrumsmannigfaltigkeiten. Univ Würzburg, Würzburg
41. Ou B, Lin Q, Du F, Jia B (2016) An extended Halanay inequality with unbounded coefficient functions on time scales. J Inequal Appl 2016(1):1–11
42. Naidu D (2002) Singular perturbations and time scales in control theory and applications: an overview. Dyn Contin Discrete Impuls Syst Ser B 9:233–278
43. Atici FM, Biles DC, Lebedinsky A (2006) An application of time scales to economics. Math Comput Model 43(7–8):718–726
44. Bohner M, Streipert S, Torres DF (2019) Exact solution to a dynamic SIR model. Nonlinear Anal Hybrid Syst 32:228–238
45. Taousser FZ, Defoort M, Djemai M (2015) Stability analysis of a class of uncertain switched systems on time scale using Lyapunov functions. Nonlinear Anal Hybrid Syst 16:13–23
46. Bartosiewicz Z (2021) Reachability and stabilizability for positive nonlinear systems on time scales. Optimization 71:3195
47. Kumar V, Djemai M, Defoort M, Malik M (2021) Finite-time stability and stabilization results for switched impulsive dynamical systems on time scales. J Franklin Inst 358(1):674–698
48. Xiao Q, Huang T (2020) Stability of delayed inertial neural networks on time scales: a unified matrix-measure approach. Neural Netw 130:33–38
49. Ali MS, Yogambigai J (2016) Synchronization of complex dynamical networks with hybrid coupling delays on time scales by handling multitude Kronecker product terms. Appl Math Comput 291:244–258
50. Lu X, Zhang X, Liu Q (2018) Finite-time synchronization of nonlinear complex dynamical networks on time scales via pinning impulsive control. Neurocomputing 275:2104–2110
51. Liu X, Zhang K (2016) Synchronization of linear dynamical networks on time scales: pinning control via delayed impulses. Automatica 72:147–152
52. Lu X, Wang Y, Zhao Y (2016) Synchronization of complex dynamical networks on time scales via Wirtinger-based inequality. Neurocomputing 216:143–149
53. Ali MS, Yogambigai J (2019) Synchronization criterion of complex dynamical networks with both leakage delay and coupling delay on time scales. Neural Process Lett 49(2):453–466

54. Wang L, Huang T, Xiao Q (2018) Global exponential synchronization of nonautonomous recurrent neural networks with time delays on time scales. Appl Math Comput 328:263–275
55. Huang Z, Cao J, Li J, Bin H (2019) Quasi-synchronization of neural networks with parameter mismatches and delayed impulsive controller on time scales. Nonlinear Anal Hybrid Syst 33:104–115
56. Kumar V, Heiland J, Benner P (2023) Exponential lag synchronization of Cohen–Grossberg neural networks with discrete and distributed delays on time scales. Neural Process Lett. https://doi.org/10.1007/s11063-023-11231-2
57. Pan L, Cao J, Hu J (2015) Synchronization for complex networks with Markov switching via matrix measure approach. Appl Math Model 39(18):5636–5649